HIGH-THROUGHPUT PHENOTYPING THAT IMPROVES THE EFFICIENCY OF A COTTON PLANT BREEDING SYSTEM

A Thesis

by

WENZHUO WU

Submitted to the Office of Graduate and Professional Studies of
Texas A&M University
in partial fulfillment of the requirements for the degree of

MASTER OF SCIENCE

Chair of Committee,	Steve Hague
Committee Members,	C. Wayne Smith
	Alex Thomasson
Head of Department,	David Baltensperger

August 2019

Major Subject: Plant Breeding

ABSTRACT

Unmanned Aerial Vehicles (UAVs) play an important role in agricultural research because they facilitate high-throughput phenotyping (HTP). Cotton (*Gossypium spp.*) is the world's leading natural textile fiber crop, and breeding programs that enhance the efficiency of growing the crop are important to the viability of the cotton industry. The effectiveness of plant breeding programs is improved when researchers have the ability to quickly evaluate important traits in a field environment. The ability to identify cotton plant height and boll count across a field can serve as an important tool in predicting plant growth and yield. In order to capture a three-dimensional (3D) view of field plots, which is believed to be helpful in estimating yield and crop development parameters, sensors mounted on UAVs must have access to a view of the ground. However, cotton planted in solid rows can obscure this view. Canopy closure prevents sensors from measuring plant architecture and boll-loads three dimensionally from the mid-growing season until the crop is defoliated. Therefore, this project was initiated to compare solid vs. skip-row planting patterns in terms of predicting yield and fiber quality since skip rows would allow UAV sensors to capture more accurate 3D data from plots. The purposes of this project were to (1) use UAVs to characterize genotype x row pattern interaction and how location and year affect that interaction, (2) evaluate the ability of UAVs to predict plant height and yield, (3) compare the accuracy of UAV-derived data from different planting patterns and (4) use images processed from UAVs to standardize data for every single row to predict yield performance. Two UAVs were used for red, green, and blue (RGB) data collection and multispectral data collection. Five cotton genotypes were grown in a skip versus solid row-pattern at three locations in 2017 and 2018. Yield and fiber qualities were measured for all

treatments. UAVs were flown across the field bi-weekly to estimate plant height, canopy cover, canopy volume, vegetation indices, open boll count and boll area over different growing stages. Without extreme weather influence, lint yield and fiber quality were not affected by Genotype X row-spacing effects. Also, year and location did not influence that interaction. In addition, yield and plant height estimations were improved when cotton was planted in a skip-row pattern. Single row rating based on orthomosaic images and 3D point cloud images correlated with yield performance. Therefore, to take full advantage of UAV data, cotton breeding programs need to plant early generation lines (progeny rows) in skip rows that allow sensors to have access to the view of the ground and capture 3D images. This can be accomplished without compromising the efficiency and accuracy of the breeding program.

ACKNOWLEDGEMENTS

I would like to thank my committee chair, Dr. Hague, and my committee members, Dr. Smith, Dr. Thomasson and special appointment Dr. Maeda. I also want to thank the UAV group from Texas A&M University-Corpus Christi. At last, I want to thank my family for their encouragement and support throughout this time.

CONTRIBUTORS AND FUNDING SOURCES

Partial financial support for this work came from Cotton Incorporated, Cary, NC. This work was supervised by a thesis committee consisting of Professor Steve Hague and Professor Wayne Smith of the Department of Soil and Crop Science and Professor Alex Thomasson of the Department of Biological and agricultural engineering.

The UAV-derived data analyzed for the results part was provided by Akash Ashapure and Anjin Chang from Texas A&M University – Corpus Christi. All other work conducted for the thesis was completed by the student independently.

NOMENCLATURE

UAV	Unmanned Aerial Vehicle
3D	Three-dimensional
HVI	High volume instrument
QTL	Quantitative trait loci
RGB	Red, green, and blue
HVI	High Volume Instrument
UHML	Upper half mean length
GWAS	Genome-wide association study
HTP	High-throughput phenotyping
G x E	Genotype x environment
GCP	Ground control point
PPK- GPS	Post Processed Kinematic GPS
PHM	Plant Height Model
DEM	Digital Elevation Model
DSM	Digital Surface Model
CC	Canopy cover
CV	Canopy volume
MPH	Maximum plant height
APH	Average plant height
NDVI	Normalized difference vegetation index
ExG	Excess green index

BIC	Bayes information criterion
RMSE	Root Mean Square Error
NAWF	Nodes above white flowers

TABLE OF CONTENTS

Page

ABSTRACT ii

ACKNOWLEDGEMENTS iv

CONTRIBUTORS AND FUNDING SOURCES v

NOMENCLATURE vi

TABLE OF CONTENTS viii

LIST OF FIGURES x

LIST OF TABLES xiii

1. INTRODUCTION 1

2. LITERATURE REVIEW 3

    2.1 Conventional breeding 3
    2.2 Value of high-throughput phenotyping 5
    2.3 The benefit of using UAV for cotton breeding 8
    2.4 The challenges for UAV applications on cotton 11
    2.5 Genotype x environment interaction 12
    2.6 Objectives and hypotheses 14

3. MATERIAL AND METHODS 16

    3.1 Trial location 16
    3.2 Genotype 16
    3.3 Field layout 16
    3.4 Harvest 17
    3.5 Data collection 18
    3.6 Data generation 22
    3.7 Visual rating 25
    3.8 Data analysis 26

4. RESULTS AND DISCUSSION 27

    4.1 UAV plant height prediction 27

4.2 UAV yield prediction 32
4.3 UAV parameters' yield predictions comparison 39
4.4 Visual ratings and actual yields comparison 46
4.5 Genotype x row patterns interaction 50
4.6 GGE biplot of least squares means of lint yield at seven individual trials 58

5. CONCLUSION 61

REFERENCES 63

LIST OF FIGURES

FIGURE		Page
1	The layout of two trials at College Station, TX	17
2	DJI Phantom 4 Pro	18
3	DJI Matrice 100	18
4	GCP location and error estimates at College Station, TX	19
5	The layout of plot boundary and grids for cotton in Corpus Christi	20
6	The layout of plot boundary and grids for cotton in College Station	21
7	Plant height model generation process	22
8	Cotton boll count and area model……	24
9	Key steps used in this study to extract data from UAV images	25
10	Comparison of UAV derived mean plant heights, manual measurement, and UAV derived maximum plant height at College Station (irrigated), TX, in 2018	28
11	Comparison of UAV derived mean plant height, manual measurement and UAV derived maximum plant height at College Station (dryland), TX in 2018	28
12	Comparison of UAV-derived mean plant height, manual measurement and UAV-derived maximum plant height at Corpus Christi, TX, in 2018	29
13	Correlation between UAV-based plant height and manual ground measurements for plant height at Corpus Christi, TX, in 2018	30
14	The relationship between UAV based- maximum plant height from different planting patterns and manual ground measurements at Corpus Christi, TX, in 2018	32
15	Correlation between manual boll count measurement and UAV-based boll count at Corpus Christi and College Station, TX, in 2018	34
16	Correlation between manual boll count measurement and Yield per row at Corpus Christi and College Station, TX, in 2018	35

17 Correlation between UAV-based boll count measurement and yield per row at Corpus Christi and College Station, TX, in 2018 35

18 Correlation between UAV-based boll area measurement and yield per row at Corpus Christi and College Station, TX, in 2018. 36

19 Correlation between UAV based-boll count from different planting patterns and yield per row at College Station, TX, in 2018 37

20 Correlation between UAV based-boll count from different planting patterns and yield per row at Corpus Christi, TX, in 2018 37

21 Correlation between UAV based-boll area from different planting patterns and yield per row at College Station, TX, in 2018. 38

22 Correlation between UAV based-boll area from different planting patterns and yield per row at Corpus Christi, TX, in 2018. 38

23 Correlation comparison between UAV data and yield throughout the whole growing season at College Station (Irrigated), TX, in 2018 39

24 Correlation comparison between UAV data and yield throughout the whole growing season at College Station (dryland), TX, in 2018..... 40

25 Correlation comparison between UAV data and yield throughout whole growing season at Corpus Christi, TX, in 2018 42

26 Orthomosaic images in the late season at Corpus Christi, TX, in 2018..... 46

27 3D point cloud displayed elevation in the middle season at Corpus Christi, TX, in 2018 ….. 47

28 Correlation between visual rating and actual yield at College Station and Corpus Christi, TX, in 2018..... 49

29 Correlation between visual rating and actual yield from different planting pattern in 2018 50

30 Least Squares Means for fiber elongation of five varieties at three locations in skip-row and solid-row patterns..... 57

31 Least Squares Means of Lint yield of five varieties at three locations in 2017 and 2018..... 57

32 Least Squares Means of UHML of five varieties at three locations in 2017 and 2018 58

33 The average-environment coordination view to show the mean performance and stability of the genotype..... 59

34 The which-won-where view of the GGE biplot..... 60

LIST OF TABLES

TABLE		Page
1	Summary of fit for the first model from stepwise at Corpus Christi, TX, in 2018	44
2	Analysis of variance for the first model from stepwise at Corpus Christi, TX, in 2018	44
3	Parameter estimates for the first model from stepwise at Corpus Christi, TX, in 2018	44
4	Summary of fit for the second model from stepwise at Corpus Christi, TX, in 2018	44
5	Analysis of variance for the second model from stepwise at Corpus Christi, TX, in 2018	45
6	Parameter estimates for the second model from stepwise at Corpus Christi, TX, in 2018	45
7	Summary of fit for the third model from stepwise at Corpus Christi, TX, in 2018	45
8	Analysis of variance for the third model from stepwise at Corpus Christi, TX, in 2018	45
9	Parameter estimates for the third model from stepwise at Corpus Christi, TX, in 2018	46
10	Visual rating and actual yield rankings at Corpus Christi, TX, in 2018	48
11	Visual rating and actual yield rankings at College Station (Irrigated), TX, in 2018	48
12	Visual rating and actual yield rankings at College Station (Dryland), TX, in 2018	49
13	Analysis of variance of yield components at 7 trials. (Row pattern x genotype interaction)	53
14	Analysis of variance of fiber traits at 7 trials. (Row pattern x genotype interaction).	54
15	Significance of main effects and their interaction in analysis of variance of yield components and fiber traits	56
16	Seven environments information	59

1. INTRODUCTION

In recent decades, genotyping capabilities have begun to out-pace phenotyping capabilities in terms of speed and accuracy. Current advances in Unmanned Aerial Vehicle (UAV) and sensor technology are now making it possible to close this gap. UAV allows fast and accurate data collection during the growing season when these platforms are equipped with appropriate sensors. The most common systems include cameras that capture red, green, and blue (RGB) bands so they produce images similar to that of the human eye. Multispectral sensors usually obtain 3 (typically including visible green, visible red and near infrared) to10 different bands in each pixel of the images, typically including visible green, visible red and near infrared, to capture both visible and invisible images of crops and vegetation. UAV can play an important role in agricultural research when incorporated with image process algorithms, visualization methods and geospatial data analysis. Leaders in this field hope to prove that such a tool would help crop breeders in identifying areas of concern in fields and other in-season field observations (Berniet et al., 2009).

Cotton (*Gossypium spp.*) is the world's leading natural textile fiber and oilseed crop. Taking field measurements manually is inefficient, laborious and likely to introduce a level of subjectivity. It is vital to evaluate whether UAV could improve the efficiency of a cotton plant breeding system since it shows the potential to measure a large number of genotypes for various traits. UAV have demonstrated that precision agriculture can be provided by various applications that focus on evaluating crop growth and vegetation (Li et al., 2012; Honkavaara et al., 2013; Lopez-Granados et al., 2016). Recent studies involving cotton and UAV images demonstrated a genotype of applications, such as monitoring cotton germination (Chen et al., 2017), estimating

cotton leaf area index (Tian et al., 2016) and predicting cotton yield in small spots (Maja et al., 2016).

The growing popularity of precision farming has created a critical need for spatial data on row spacing (Geesing et al., 2014). In order to capture a three-dimensional image, sensors mounted on UAVs must have access to the view of the ground, but cotton planted in solid rows may obscure this image. A confounding issue that cotton breeders have encountered is the prohibition of sensors from measuring plant architecture and boll-loads three-dimensionally by canopy closure from the mid-growing season until the crop is defoliated. Thus, one of our hypotheses is that solid row data processed from orthomosaic images may not be as accurate as data from skip-row planted cotton.

In the meantime, breeders hope to make sure that skip rows will not affect the evaluation of progeny rows. This project compared solid vs. skip-row patterns in terms of predicting yield and fiber quality since a skip-row pattern would allow UAV sensors to accurately capture 3D data from plots. Our analysis focused on lint percent, lint yield, and fiber quality characteristics including micronaire, UHML, length uniformity, strength and elongation.

2. LITERATURE REVIEW

2.1. Conventional breeding

2.1.1. Introduction

Conventional plant breeding is the improvement of crop populations using traditional tools. Human selection serves an important role in this breeding process. The use of visual selection in the 1700s was the first method of cotton improvement in the USA and led to the development of adapted, successful cotton (*Gossypium hirsutum L.*) cultivars (Niles and Feaster, 1984). Plant visual selection made by breeders would accelerate breeding progress and gradually change the phenotype towards the desirable characteristics according to a breeder's purpose (Bernardo, 2003). For example, Meredith and Bridge (1973) proved that by selecting F2 plants with higher yield potential, the F3 generation yielded 5.7% more lint than randomly advanced plants and those lines selected specifically for fiber strength.

Furthermore, electronmechanical instruments have been used for many years in an attempt to help breeders make selections. For example, cotton breeders can make a more accurate and efficient selection using High Volume Instrument (HVI), which measures upper half mean length (UHML), fiber strength, elongation, micronaire, length uniformity index and can also quantify color and leaf trash.

Conventional breeding utilizes processes that emphasizes improvements in traits that are not new for the species. Those characteristics have been present for millennia within the gene pool of the species rather than adding new genes to the genome of a plant.

2.1.2. Challenges for conventional breeding

One consideration for most cotton breeding programs is the physical limitation of how many individual plants, progeny rows, and strains can be evaluated and harvested each season. Thus, prior to harvest, breeders need to quickly evaluate and select superior lines for advancement. The effectiveness of field-based visual selections may also be associated with breeder's experience. For example, Bowman et al. found in 2004 that breeders with more than 30 years of experience had a greater likelihood of selecting plants or cultivars with improved lint yield than those breeders with less experience. Additionally, Byth et al. (1969) found plant height and cotton maturity can impact the breeder's judgment as well.

Because of the limitations of conventional breeding, new techniques based on molecular breeding are playing an increasingly important role in cotton improvement. Development of molecular markers improved the efficiency and speed of plant breeding programs which integrated traditional and molecular techniques. DNA marker studies in multiple and large plant populations enable researchers to identify quantitative trait loci (QTL) linked with traits of interests (Shen et al. 2006). Efficient and inexpensive markers associated with desirable traits such as drought tolerance or yield can facilitate efficient and rapid marker-assisted selection in cotton. Fang et al. (2017) used a genome-wide association study (GWAS) with gene-based association to rapidly identify candidate genes associated with cotton lint yield. Those genes were isolated and sequenced to perform haplotype-based analysis. Results showed that preferred haplotypes increased lint percent and number of bolls per plant by 11.3% and 4.4% respectively. These findings could reduce the time and increase the accuracy of selecting desirable traits when compared with conventional breeding.

In recent decades, genotyping capabilities have begun to out-pace phenotyping capabilities in terms of speed and accuracy, but current advances in UAV and sensor technology are now making it possible to close this gap because they facilitate High-throughput phenotyping **(**HTP), which enables efficient measurement of complex traits for a larger sample size.

2.2. Value of high-throughput phenotyping

2.2.1. Background

The first earth observation satellite was launched in April 1960 as the first of a series of experimental weather satellites designed to monitor cloud pattern. After about thirty years，SPOT-4, with the most important advanced "Vegetation" instrument, was launched to allow continuous and worldwide crop monitoring (Campbell and Wynne, 2011). Satellites have been used to evaluate crop growth for decades, but their spatial resolutions are generally inadequate for precision agriculture. In addition, the acquisition of data from satellite sensors is dependent upon the platform's orbit characteristics and cloud occurrence.

In terms of UAVs, they were initially used for chemical spraying since they could overcome obstacles encountered by ground applicators or even manned aerial applicators such as poor lying conditions or tall crops such as sorghum (Sugiura et al., 2005). With the development of sensor technologies, airborne remote sensing has the capability of rapid image acquisition, which allows aerial vehicles to fly at a date close to specific phenological stages at ideal crop stages. Additionally, they can fly at lower altitudes than regular aircraft to perform specific field investigations with high precision.

Nowadays, the versatility and flexibility of a UAV allow easy access to customize spatial, temporal, and even spectral resolutions (Colomina and Molina, 2014). In order to fly

with minimal weight and maneuverability, light composite materials are used in the construction of UAV. Diverse navigation systems or sensors such as an RGB sensor or multispectral sensor are integrated with the vehicle. Images from UAV can be processed with image processing algorithms, visualization methods and geospatial data analysis to maximize their potentials. After UAV data collection, eospatial data, such as 3D point clouds and orthomosaic images, were generated by reconstructing the 3D structure from a series overlapping and offset images without ground control points and automation using Structure from Motion (SfM) (Campbell and Wynne, 2011). Through automatic location of matching features, camera positions and poses are automatically solved without the need for ground control points. Orthomosaic images generated from SfM can provide breeders more accurate information without geometric errors to predict biomass, disease, lodging and stress. Thus, remote sensing can be involved in data collection, field variability mapping and aid in the decision-making process (Stafford, 2000).

2.2.2. Vegetation indices

Remote sensing of vegetation mainly uses passive sensors to obtain electromagnetic wave reflectance from canopies. Visible light including (red) wavelengths are largely absorbed by pigments in plant leaves while near-infrared wavelengths are strongly reflected by leaves. These reflectance properties are determined by morphological and chemical characteristics of the leaves' surface but will change over different growing stages (Campbell and Wynne, 2011). Vegetation indices are used to transform spectral data into a single value for each pixel on the image in order to improve vegetation classification, crop management, and disease investigation, which accelerates applications of UAVs in agriculture.

There are many vegetation indices designed to maximize sensitivity to the vegetation characteristics while minimizing confounding factors such as soil background reflectance or

atmospheric effects, but the most widely used is normalized difference vegetation index (NDVI), which was initially developed to use Landsat spectral data to globally assess agriculture and forestry (Tucker, 1979). NDVI is calculated using the ratio of the reflectance in the near-infrared and red light of the electromagnetic spectrum ($NDVI = \frac{(NIR + Red)}{(NIR - Red)}$). NDVI provides reliable results from different growth stages because it is able to mitigate topographic effects and variations in the sun illumination angle and other atmospheric elements such as haze. NDVI is commonly used and widely confirmed to correlate with plant health and leaf area. Sudbrink (2003) reported that damage to cotton plants from beet armyworms *Spodoptera exigua* (Hubner), corresponded to lower NDVI when data was gathered from remote sensing images. This relationship between beet armyworm damage and NDVI was the result of plants losing vigor and loss of leaf area.

However, NDVI is not sensitive enough to the leaf-color change from green to yellow or red because green reflectance is not used in the calculation of NDVI. When evaluating vegetation cover at low flying height, Excess Green Index (ExG) that uses the full visible light spectrum (green, red and blue) has a better performance than NDVI (Nijland et al., 2014). This type of vegetation index can more easily distinguish plants from background soil than NDVI, using the formula ExG = 2 x Green – Red – Blue, to provide an intensity image with approximate nearbinary outline of plant regions of interest (Woebbecke et al., 1995). Mao (2003) used the ExG to successfully detect between-row weeds and proved ExG index can separate plants from soil and withered plant residue. Thus, these two vegetation indices were used in this project.

2.2.3. Recent applications of UAV

The use of UAVs is growing rapidly across different application domains including civil infrastructure inspection, precision farming and remote sensing. Recently, agricultural studies have explored UAV platforms carrying diverse sensors to monitor the status of crop growth throughout the growing season (Rasmussen et al., 2013; Gevaert et al., 2015). The agricultural applications of UAVs are usually concentrated on low flying height operations over small areas within a field for precision farming.

In general, agricultural applications using remote sensing include classification of crop species (Rao et al., 2008), management of pests (Lan et al., 2009), analysis of leaf area index and chemical content (Wu et al., 2007), and identification of plant water stress and control of weeds (Gutiérrez-Peña et al., 2008). Additionally, this technology was used on a large variety of crop species such as canola, corn, cotton and sorghum (Seelan et al., 2003). Recent agricultural studies utilizing UAV images on cotton have demonstrated a variety of applications, such as monitoring cotton germination (Chen et al., 2017), estimating cotton leaf area index (Tian et al., 2016) and predicting cotton yield in small spots (Maja et al., 2016).

2.3. The benefit of using UAV for cotton breeding

2.3.1. Plant height prediction

Among various phenotypes, plant height is an important phenotypic trait, which can be used as an indicator of overall plant growth. In addition, repetition of plant height measurements is critical to estimate growth rate, flowering and boll set, and overall maturity stages. With such information, plant breeders can select genotypes well-adapted to their commercial regions of interest. Furthermore, plant growth rate or plant height can be used to predict plant health status

and yield potential (Sui et al., 2001). Therefore, measuring plant height is of great interest to breeders, and it can be done manually with measuring sticks or tapes or hand-held instruments. However, manual measurements are not suitable for large field due to the fact that they are time-consuming and labor-intensive.

As mentioned earlier, UAVs can provide rapid, continuous and precise data collection, which would be beneficial for breeders' understanding of the influence of external conditions on plant performance throughout crop development. 3D point cloud data can generate a digital surface model of objects' upper surface, like the top surface of crop plants. Plant height can be estimated by subtracting the digital elevation model of the soil surface from the digital surface model when the plants are growing. Several studies have evaluated the capability of SfM for estimating height of sorghum and maize (Shi et al., 2016; Malambo et al., 2018). Those studies show a new avenue to enhance plant research programs through SfM and UAV. Therefore, it is imperative to evaluate the ability of UAVs to predict cotton plant height.

2.3.2. Seed cotton yield prediction

Crop yield is perhaps the most important information for crop management in precision agriculture. Regression analysis suggests a significant linear relationship between lint yield and open boll count on a meter basis (E.R. Norton, 1999).

Typically, yield prediction is conducted by counting bolls, which is tedious and misleading without considering other factors that may influence final yield. Also, such estimation is mostly based on farmers' visual inspection and experience, likely without a scientific basis. Therefore, predicted yield could be very different from the actual yield. Accurate estimations or predictions of cotton yield are important because cotton yield is the result of cotton growth and production management.

Cotton yield can be affected by many external factors. Low yields can be the result of harvesting immature crops with many immature fibers, which contributes to less revenue to the producer and a lower quality product to market (Snipes and Baskin, 1994; Bange et al., 2010). Yet harvesting a crop much later than its maturity date also leads to loss of yield and crop quality due to the effects of weathering (Williford, 1992; Bednarz et al., 2002). Therefore, it is vital to develop methods to accurately predict crop maturity and yield, which may be done using a UAV. Jung et al. (2018) proposed a new algorithm to analyze open cotton boll count and area. The red band of an orthomosaic image was used for binary classification to separate cotton boll from backgrounds. The extracted the number of open bolls, average area of open bolls, average diameter of open bolls, perimeter of open bolls, perimeter to area ratio were used to performed selection. Minimum and average lint yield were increased using UAV selection by 7.4 % and 10%. This study provides a powerful tool for breeders to accelerate yield selection progress.

2.3.3. Visual selection through UAV images

Moreover, plant architecture can affect plant quality, adaptability and yield. Cotton plant architecture is important because it may influence mechanical harvest effectiveness and yield. Plant architecture refers to a series of major traits which include main stem height, number of nodes on the main stem, internodal length and number of fruiting branches (Azhar et al. 1999). One of the previous studies about the effect of morphological traits on yield demonstrates that bolls per plant were highly significantly correlated with yield, and the number of sympodial branches had an effect on cotton yield per plant (Farooq et al. 2013, Hazeem et al. 2005). Also, plant canopy structure can strongly affect crop functions such as yield and stress tolerance, and canopy size is an important aspect of canopy structure. Therefore, phenotypic evaluations using UAV based on plant morphological traits and canopy architecture may become important in

cotton production. However, accessible studies have shown limited useful information related to yield potential, so more studies need to be done to better understand yield potential factors based on UAV remote sensing.

2.4. The challenges for UAV applications on cotton

Although UAVs can improve high-throughput phenotyping, precision farming has also created a critical need for spatial data on row spacing and related soil characteristics (Geesing et al., 2014). For example, one previous study suggested that the accuracy of processed data from SfM may be influenced by canopy structure (Malambo et al., 2018). The biggest challenge for UAV applications on cotton is canopy closure, which is the amount of ground surface shaded by cotton canopies as seen from above. In order to capture accurate three-dimensional images, the sensor mounted on the UAV should have a view of the ground. However, cotton planted in a solid-row pattern may obscure the ground and important parts of the plant. Canopy closure will likely prevent the sensor from measuring plant architecture and boll-load three-dimensionally, especially from mid-growing season until the crop is defoliated.

An alternative planting pattern, skip row configuration, which is to plant one row and then skip one row, may solve this problem. The empty row could provide a view of ground elevation and decrease the possibility of overlapping canopy closure. This planting pattern may increase the accuracy of UAV data produced from orthomosaic images and 3D point cloud images.

2.5. Genotype x environment interaction

2.5.1. The importance of yield and fiber quality

If a skip-row pattern can increase the accuracy of UAV data generated from orthomosaic images and 3D point cloud images, how does skip row affect the evaluation of cotton progeny rows? Breeders are more concerned with lint yield and fiber traits because lint yield is the most important factor for producers aiming to maximize profit while fiber traits determines final product quality at spinning mills.

Lint yield is the most important consideration in cotton production programs to maximize profit. There are multiple lint yield components, such as the number of bolls per plant, boll weight and lint percent, which represents the proportion of lint weight to seed cotton weight, and can be influenced by the boll size, seed size and the number of seeds per boll (Culp and Harrell, 1975).

Although a high-yield of fibers is desirable, fiber quality properties are important for predicting the value of the raw cotton product. Also, improvements of fiber quality are essential for meeting demands of the textile industry. The HVI system is widely used to evaluate fiber quality properties, which includes UHML, fiber micronaire, strength, elongation and length uniformity. All of these fiber traits are important in determining fiber quality. One previous study proposed that UHML is widely used as the standard to determine fiber length (Smith et al., 2009), which is an important determinant of yarn quality and processability. Micronaire measures air permeability of compressed cotton fibers, which is an indication of fiber maturity and fineness. It is associated with mill processing performance and quality of the end products. Fiber strength denotes the maximum tension of a bundle of fiber is capable of sustaining before breaking while fiber elongation is the extension of the bundle of fibers before rupture. Better

tensile properties tend to lead to producing stronger spun yarns and higher quality finished textiles. The current marketing system rewards the varieties with higher strength and higher elongation, because these cottons tend to receive a premium price. Length uniformity is the ratio of the average length to the UHML, typically shown as a percentage, and it results from the genetic potential of a variety as well as fiber breakage during harvesting and ginning. High length uniformity is preferred by the textile industry because it indicates a higher quality product and improves of textile processing efficiency.

2.5.2. The influence of row pattern on cotton yield and fiber quality

Fiber yield and quality can be influenced by many external factors. Previous studies have shown that different row patterns have different effects on cotton growth. Compared with the conventional row pattern (solid row), plants in skip-row pattern would continue more rapid growth and reproduction longer than cotton in solid-row patterns during dry periods because the skip-row pattern enable plants to extract more moisture by increasing the soil volume available per plant (Nichols et al., 2004). This pattern increases the yield if conditions improve and minimizes the potential fiber quality decrease if conditions deteriorate (Dong et al., 2006). For example, Jones (1997) found dryland cotton from a skip-row pattern had 21.8% greater boll production and 25.4% more lint yield when compared to cotton from a solid-row pattern. Also, cotton plant height and maturity have been improved by using skip-row patterns (Jones, 1997; Marois et al., 2004). On the other hand, canopies of solid-rows are likely to close earlier and more completely to deter weed growth, and mature earlier than those of skip-row patterns. But this effect diminishes with narrower rows (Gwathmey et al., 2007). According to the results from previous studies, the skip-row pattern could reduce production costs and improve plant

development and improve yield per planted hectare, making this planting method an economically viable planting-pattern alternative in dryland cotton production areas.

Row spacing is also critical in regulating fiber quality. Meng et al. (2016) found that fiber micronaire, fiber maturity ratio and fiber fineness decreased when row spacing increased while fiber length, fiber uniformity index, fiber strength and fiber elongation were insignificantly influenced by row spacing.Water deficiency late in flowering period has a negative influence on fiber length and fiber elongation (Hearn, 1976). In this case, fiber length and elongation would benefit from skip-row planting pattern since it provides more soil volume from which the plant can extract moisture. In addition, nutrient deficiencies would impact fiber quality, especially fiber length (Sawan et al. 2006). Because of less competition for nutrient in the skip-row pattern, fiber length from skip-row pattern may outperform those from the solid-row pattern.

Phenotypic variations are caused by interactions between the environment and genes' expression that affect the trait of interest. Genotype stability for trait performance is a direct measure of the presence and effect of genotype × environment interactions (G x E interactions), which result from the differential performance of a genotype or cultivar across environments (Campbell, 2005). Many important agricultural traits are end-point measurements because they demonstrate the combined effects of large numbers of genes acting independently and together. The investigation of G x E interactions is a concern and challenge for plant breeders due to the diverse elements of the environment, such as temperature, pest complexes, soil pH, moisture, etc.

2.6. Objectives and hypotheses

The objectives of this study are to (1) use UAVs to characterize genotype x row pattern interaction and how location and year affect that interaction, (2) evaluate the ability of UAVs to

predict plant height and yield, (3) compare the accuracy of UAV-derived data from different planting patterns and (4) use images processed from UAVs to standardize data for every single row to predict yield performance. The hypotheses for this research are: (1) Row-spacing (solid vs. skip-row) has no effect upon lint yield or fiber quality; (2) UAV can accurately predict plant height (R^2>0.94) and yield (R^2>0.85); (3) UAV data generated from orthomosaic images and 3D point clouds, such as plant height and boll count from skip rows is more accurate than from solid rows; (4) Single row rating based on orthomosaic images and 3D point cloud images correlated with yield performance.

3. MATERIALS AND METHODS

3.1. Trial location

The field experiment was conducted at Weslaco (irrigated), Corpus Christi (dryland) and College Station (irrigated) in 2017. The 2018 trials occurred at Weslaco (irrigated), Corpus Christi (dryland), College Station (irrigated) and College Station (dryland). Cotton was planted at Corpus Christi, Weslaco and College Station on 22 March, 18 March and 26 April in 2017 and on 14 March, 16 March and 03 May in 2018 respectively.

3.2. Genotype

The experiment involved five genotypes: 'Tamcot 73' (early maturing variety) (Smith et al., 2011; PI 662044)), 'Tamcot 211' (okra-leaf), 'Tamcot 421' (mid-maturity), 'TAM exp. T-08' (full-season; high-quality fiber) and 'TAM exp. X-26-3' (drought tolerant; high-quality fiber)

3.3. Field layout

The trial design was a split-plot of a randomized complete block design. Row spacing was the main-treatment and genotype was the sub-treatment. The five genotypes were planted in both a skip-row pattern (every-other row was blank) and a solid-row pattern in 2017 and 2018 at three locations. Each entry was replicated four times. There are two rows in each solid-row plot and one row in each skip-row plot. The row spacing at Weslaco and Corpus Christi was 96 cm and 192 cm for solid-row patterns and skip-row patterns, respectively. The row spacing at College Station was 102 cm and 206 cm for solid-row patterns and skip-row patterns, respectively (Figure 1). These row spacings were the same for each location during both years.

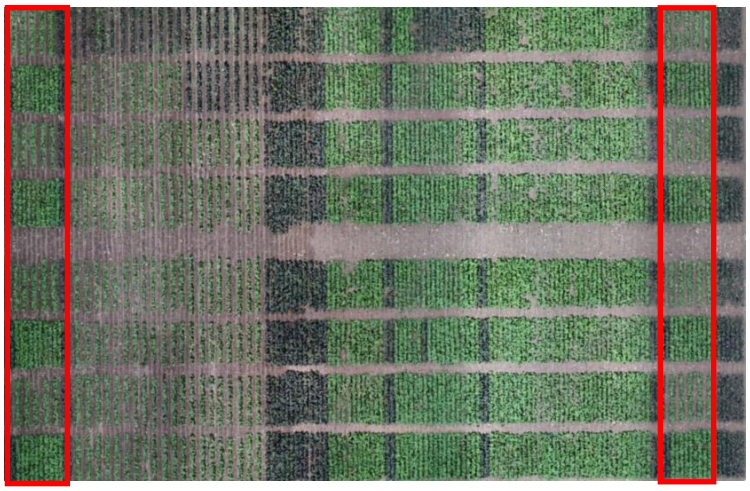

Figure 1: The layout of two trials at College Station, TX. (Left: Irrigated; Right: Dryland).

3.4. Harvest

The experiments were harvested at Corpus Christi, Weslaco and College Station on 31 July, 02 August and 02 October in 2017 and on 31 July, 06 August, and 17 November in 2018, respectively. Seed cotton harvested with a mechanical plot picker harvester and seed cotton yield (kg/ha) was calculated using the formula: $\frac{\text{Seed cotton weight per plot (kg)}}{\text{Plot area (ha)}}$.

From each solid row and skip row pattern plot, a 30-boll sample from the left row was hand harvested at Corpus Christi, Weslaco and College Station in 2018 and at College Station in 2017. Of the four replications, two of them were randomly hand harvested at Weslaco and Corpus Christi in 2017. As before, 30-boll samples were taken. Samples were weighed and ginned on a 10-saw laboratory gin without cleaner for lint percent calculation. Lint percent for each plot was calculated from the ratio of seed cotton weight and lint weight, using the formula: $\frac{\text{lint weight}}{\text{seed cotton weight}}$ x 100. A lint sample (50 gram) from each plot was sent to Texas Tech University's Fiber and Biopolymer Research Institute at Lubbock, Texas, for HVI analysis, the left row from each solid-row pattern plot was harvested with a mechanical

cotton picker harvester and seed cotton was weighed to estimate lint yield (kg/ha) using the formula: seed cotton yield (kg/ha) x lint percent. The same process was repeated for skip-row pattern plots. These yield and fiber traits data from Weslaco, Corpus Christi and College Station in 2017 and 2018 were used to investigate genotype x row pattern interaction.

3.5. Data collection

Figure 2: DJI Phantom 4 Pro.

Figure 3: DJI Matrice 100.

UAV platforms equipped with sensors were used to collect data over the test field on a bi-weekly basis during the growing season with a similar protocol at Corpus Christi and College Station in 2018 to investigate if UAVs are able to improve the efficiency of cotton breeding programs. Two different UAVs were used for Red- Green- Blue (RGB) data collection and multispectral data collection. To collect RGB data, a DJI Phantom 4 Pro was equipped with an RGB sensor, the standard 20MP gimbal-stabilized DJI sensor (Figure 2). To collect multispectral data, a SlantRange 3P and Micasense RedEdge were integrated with DJI Matrice 100 platform (Figure 3). Autonomous flight missions were performed based on the following conditions at College Station for RGB sensor and multispectral sensor respectively. The RGB sensors,

equipped with UAV, captured images at a 30-meter altitude with 80% to 90% forward overlap and side overlap, resulting in about 550 raw images over the study area. The multispectral sensor, attached to the UAV, was flown at an altitude of 50 meters with 60% to 70% forward overlap and side overlap, resulting in about 4000 raw images over the study area. The same flight missions were done at Corpus Christi, but the only difference was the number of total raw images were about 350 and 700 for RGB and multispectral sensor, respectively, due to the different sizes of the fields.

Figure 4: GCP Location and error estimates at College Station, TX.

Wooden panels were constructed with a cross pattern to use as Ground Control Points (GCP) (Figure 4). The center of nine GCPs was measured by Post Processed Kinematic GPS (PPK- GPS) system, model 20 Hz V-Map Air (Micro Aerial Project L.L.C., Gainesville, FL), which can provide a sub-centimeter location accuracy. Coordinates of the ground target points were inserted into Photoscan for geo-referencing. Row images were processed using Agisoft

Photoscan Professional version 1.2 (Agisoft LLC, 11 Degtyarniy per., St. Petersburg, Russia). SfM was used to generate geospatial data products. In SfM processing, key points from a series of overlapping images are identified by using scale invariant feature transform (SIFT). Interior and exterior orientation parameters are computed from those key points identified before by using block bundle adjustment. Deploying densification, a dense point cloud can be constructed to build digital surface model (DSM). Finally, the DSM is used to project every image pixel to generate an orthomosaic.

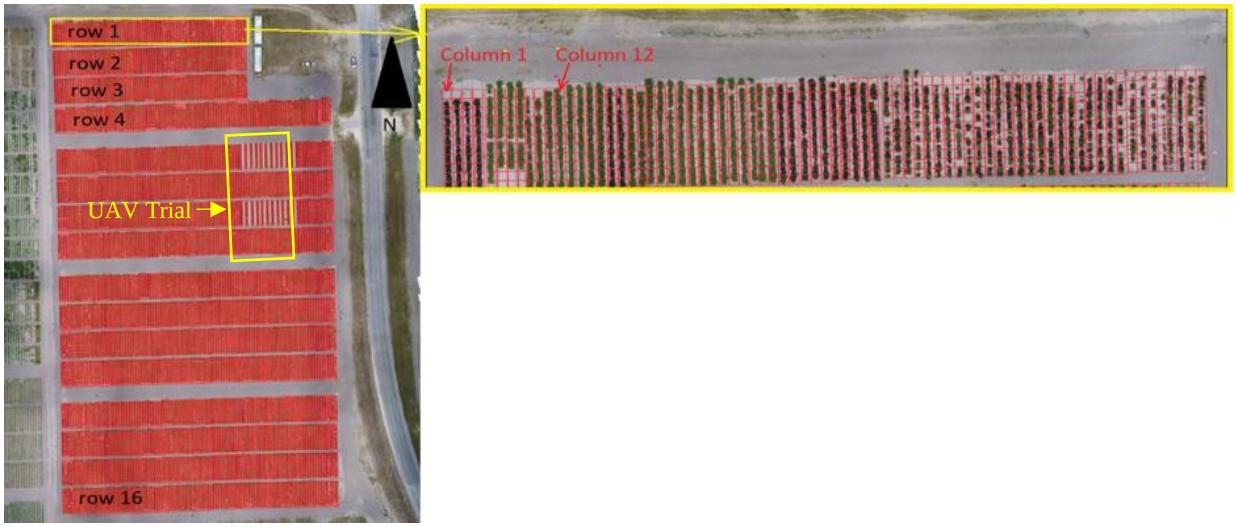

Figure 5: The layout of plot boundary and grids for cotton in Corpus Christi, TX.

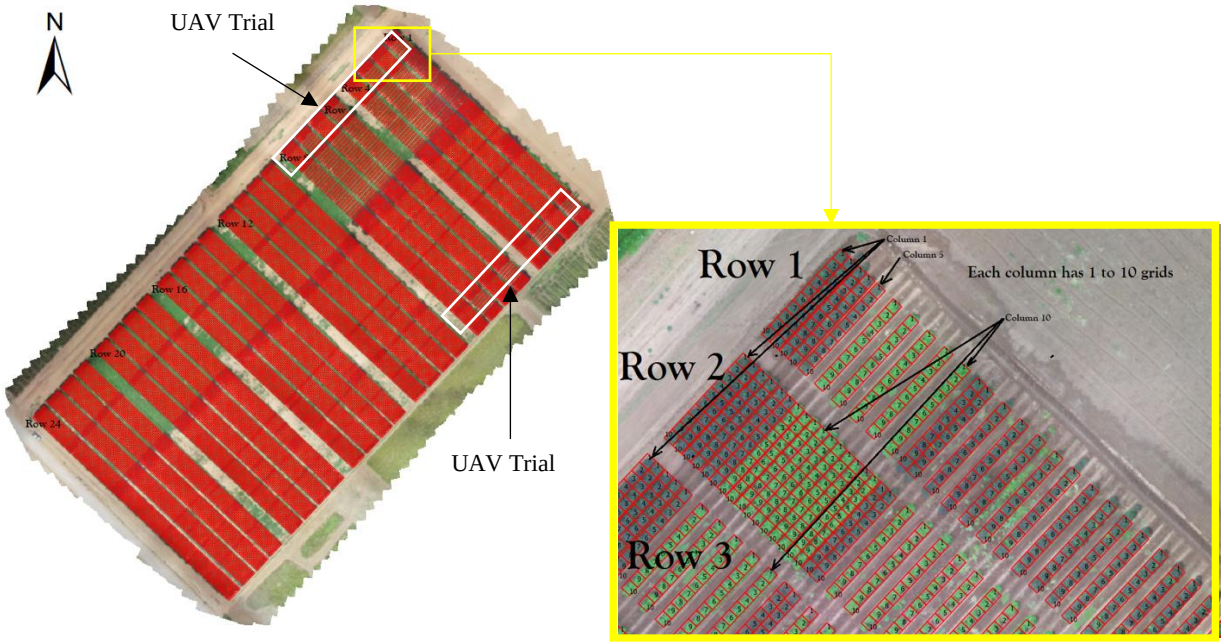

Figure 6: The layout of plot boundary and grids for cotton in College Station, TX.

Whole fields on the orthomosaic images were divided into a row, column and grid format. As can be seen in figure 5, 16 rows are further divided into columns (each column is a single cotton plot) and each column is divided into 11 grids of 0.9x1 meter at Corpus Christi. The same procedure was performed at College Station. Ten grids of 0.95x1 meter per row were designed along the planting rows to extract data at College Station (Figure 6).

In the meantime, ground manual measurements were collected. Plant height was measured as the shortest distance between the upper boundary of the apical terminal and the base of plant. Five random plants were measured per plot at College Station and Corpus Christi in 2018. Plant heights were measured 8 times from 24 April to 10 July at Corpus Christi and 6 times from 16 July to 20 August at College Station. In addition, boll counts per meter were measured in each plot just prior to harvest at College Station and Corpus Christi in 2018, which enabled us to estimate the number of bolls for the entire plot. Boll count per meter was measured on 31 July just prior to harvest at Corpus Christi. Boll count per meter was measured on 01

September at College Station, but due to excessive rain, cotton was not harvested until 17 November.

3.6. Data generation

All the parameters generated from SfM were converted into a grid-wise measurement. 3D point cloud data can generate a digital surface model, which provides the surface with the elevation of objects in the field. The Plant Height Model (PHM) was generated by subtracting the Digital Elevation Model (DEM) from the Digital Surface Model (DSM) for each flight date (PHM=DEM-DSM) as described by Chang et al. in 2018 (Figure 7). The maximum plant height within each grid was used as the representative point for plant height in the grid to avoid situations in which height values from the middle of the crop or non-crop pixels such as ground were selected. Additionally, average plant height was generated for each grid. During this process, in order to remove ground effect, values above 10 cm were averaged and those below 10 cm were discarded around 30 days after planting.

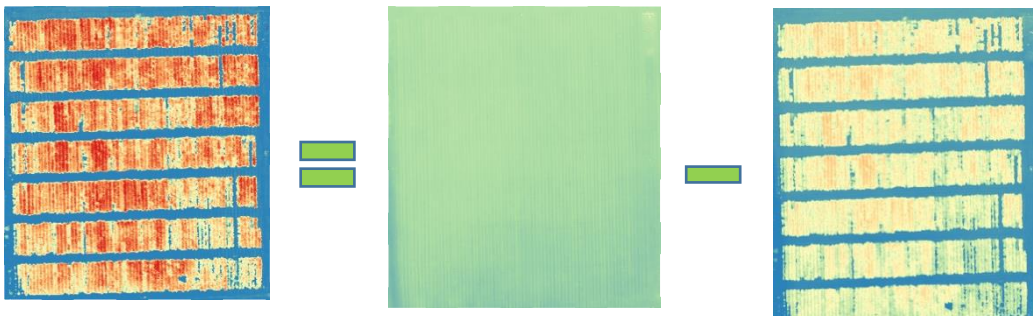

Figure 7: Plant height model generation process. (Left: Plant height model; Middle: Digital Elevation model; Right: Digital surface model).

ExG, NDVI, canopy cover (CC) and canopy volume (CV) were calculated using orthomosaic images taken from RGB and multispectral sensors, using the following equations:

$$\text{NDVI} = \frac{(\text{NIR} + \text{Red})}{(\text{NIR} - \text{Red})}$$

ExG = 2 x Green – Red – Blue

$$CC_{RGB} = \frac{[(\sum Pixel\ size^2), if\ canopy]}{\sum(Pixel\ size^2)} * 100$$

$$CC_{NDVI} = \frac{[(\sum Pixel\ size^2), if\ NDVI > 0.6]}{\sum(Pixel\ size^2)} * 100$$

$$CV = \sum(Hi \times Pixel\ size^2)$$

Only NDVI pixel values equal to or greater than 0.5 were used to estimate the average NDVI, enabling the discarding of pixels representing the soil. Similarly, only ExG pixel values equal to or greater than 0.2 were included to estimate average ExG for the same reason. CC represented the percentage of canopy cover per grid using the multispectral sensor and RGB sensor, respectively. As seen on the equation for CC_{NDVI}, NDVI values higher than 0.6 were considered as part of the canopy. After building the DEM, CV can be generated. CV represents the canopy volume in cubic meters and Hi represents the pixel value in the DEM, which is the height of the i^{th} pixel within the grid.

Because of the low altitude flight pathway and high resolution captured by sensors, it is possible to delineate cotton bolls from background images within the orthomosaic image. The proposed methodology of Yeom et. al (2018) was used in this project. The first step is to select cotton boll candidate from the background. Random seed points were extracted and a region growing algorithm was used on each subset image. Based on collective spectral information of cotton boll candidates, Otsu method which is used to automatically perform clustering-based image thresholding was applied to determine the brightness threshold in order to differentiate cotton bolls from background. Finally, a binary classification was displayed by applying the derived threshold value to the orthomosaic image (Figure 8). The patch size analysis was used to

calculate the total number of open boll and open boll area in each grid. Figure 9 shows the key steps of image and data processing used in this project.

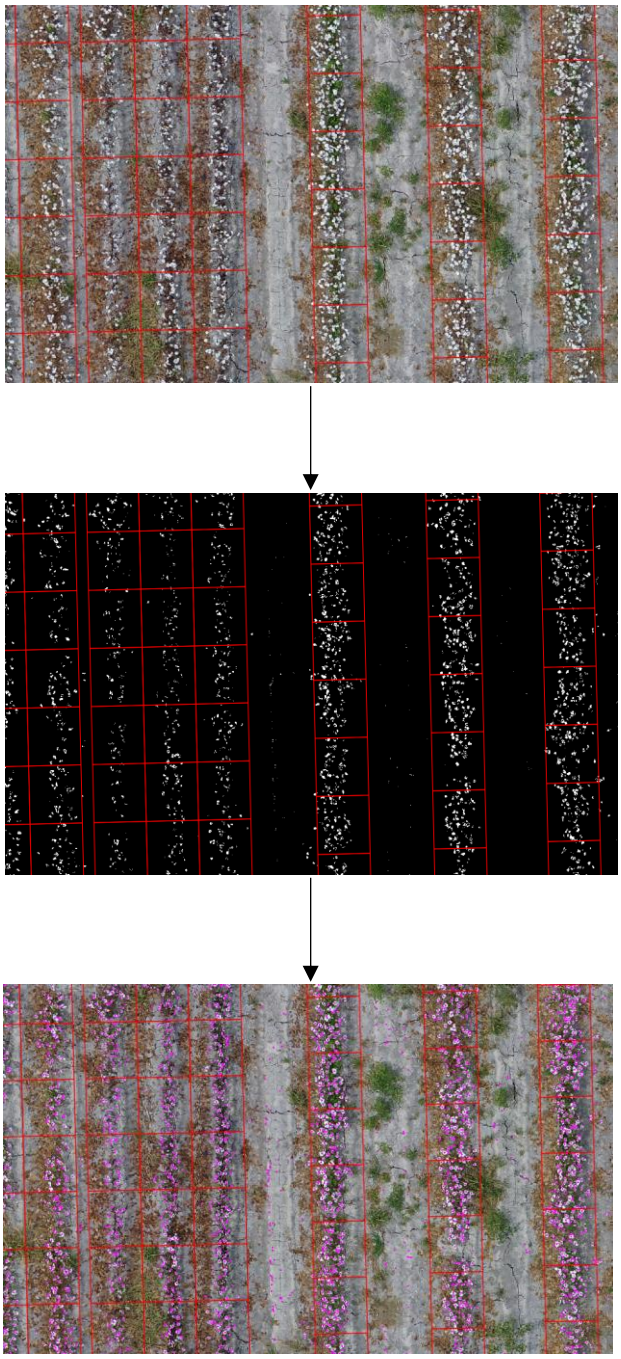

Figure 8: Cotton boll count and area model. (First: RGB image; Second: Binary classification; Third: Patch size analysis).

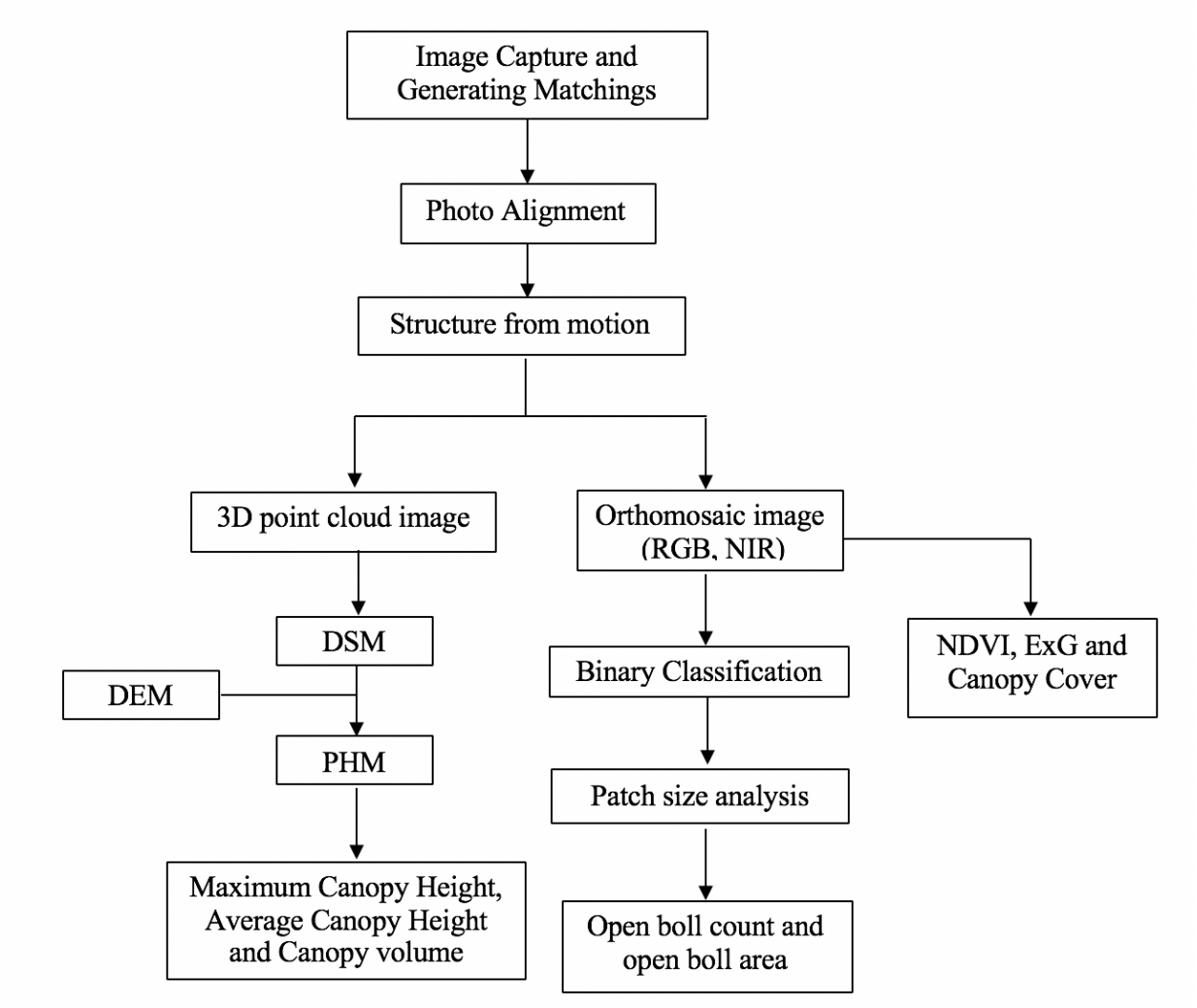

Figure 9: Key steps used in this study to extract data from UAV images.

3.7. Visual rating

Based on orthomosaic images and 3D point cloud images, single row was manually rated from 1 to 7 from planting to harvesting so that these estimates could be related to measured lint yield. Visual rating for each single row was performed based on orthomosaic images and 3D point cloud images of 10 different dates at Corpus Christi and 12 different dates at College Station, respectively. In early season, ratings would focus on germination rate, plant height and CC. In middle season, the focus would change to plant height, CV, the number of flowers and

plant health. In the late season, our focuses for the rating are the number of cotton bolls, plant health and CC.

3.8. Data analysis

UAV-derived data were processed in 2018 at College Station and Corpus Christi. Regression analysis using SAS v.9.4 (SAS v.9.4, SAS Institute, 2015) and JMP®, Version 13 Pro (SAS Institute Inc., Cary, NC, 1989-2019) was performed to compare ground truth data with UAV-derived data in order to evaluate the ability of UAV remote sensing to estimate plant height and boll count. In addition, the accuracy of UAV-based data from different row patterns was compared using the same method. The correlation between visual ratings of every single row and actual yield was investigated using regression analysis.

Furthermore, variances were analyzed to characterize genotype x row pattern interactions and how location and year affected those interactions using fiber traits and yield data in 2017 and 2018 at Weslaco, College Station and Corpus Christi Also, Genstat (16th Edition. VSN International, Hemel Hempstead, UK) was used to generate GGE biplot.

4. RESULTS AND DISCUSSION

4.1. UAV plant height prediction

4.1.1. Comparison of UAV-derived plant height and manual measurement

UAV-based mean plant height data and maximum plant height data were extracted from 3D point cloud over the growing season and averaged for each plot. Five random manual measurements were also averaged for each plot. Although ground truth data from six dates were measured, there were problems with the GPS on 10 August and 22 August, which lead to incorrect vertical accuracy at College Station. Therefore, only four days of manual and UAV-based plant heights were compared at College Station. In addition, because of environmental factors, cotton plants at College Station were taller than cotton plants at Corpus Christi by mid-season, which ultimately resulting in lodging at College Station. Lodging was exacerbated at College Station due to strong winds and rain in mid-August. In order to measure the height of these plants, they were manually lifted off the ground. As a result, UAV-based plant heights were shorter than ground truth plant heights at College Station (Figures 10 and 11).

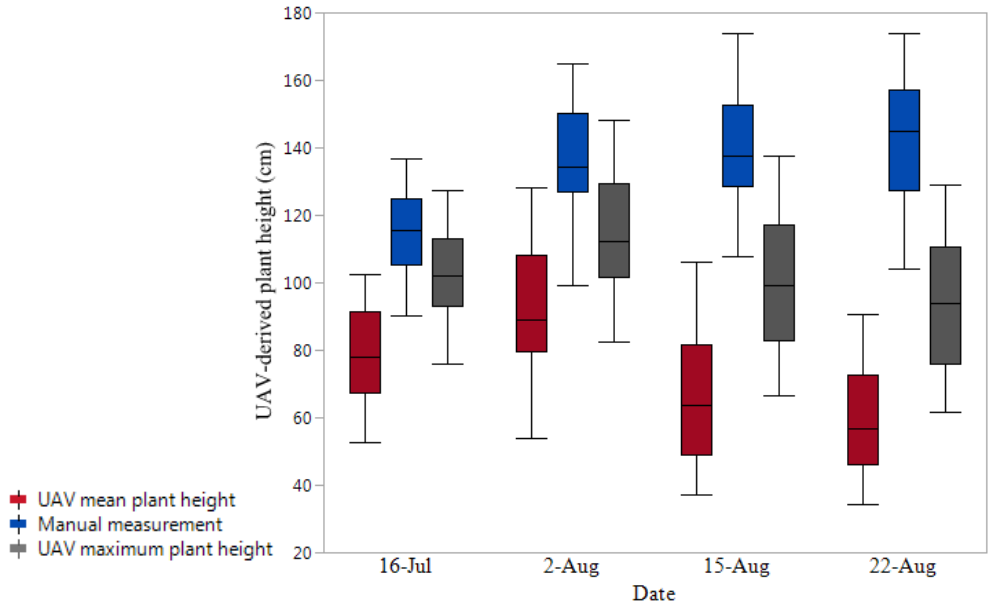

Figure 10. Comparison of UAV derived mean plant heights, manual measurement, and UAV derived maximum plant height at College Station (irrigated), TX, in 2018.

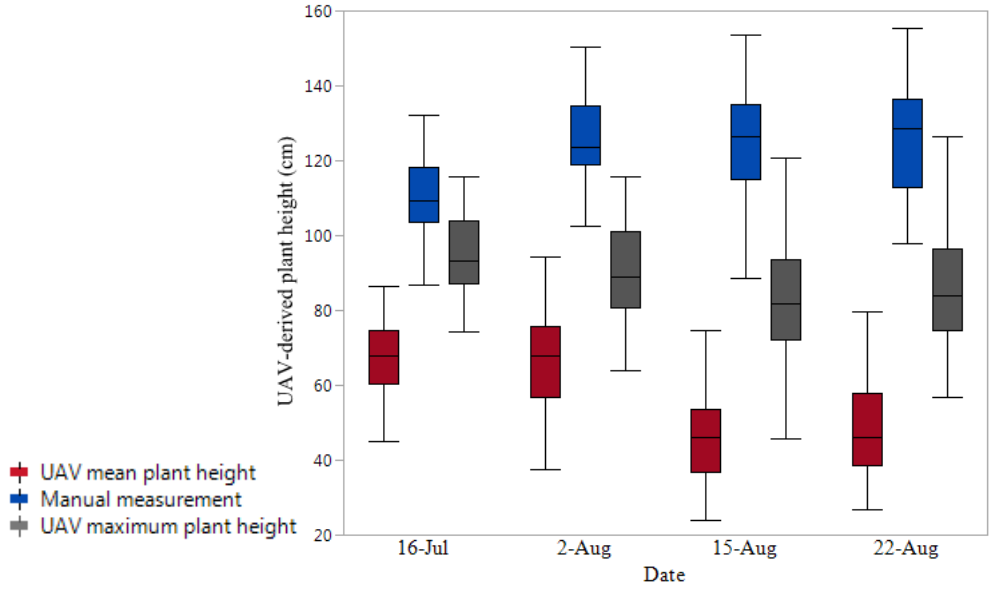

Figure 11. Comparison of UAV derived mean plant height, manual measurement and UAV derived maximum plant height at College Station (dryland), TX in 2018.

Plant height estimates at Corpus Christi were not complicated by lodging. There was a tendency for UAV-based mean plant height to underestimate plant height at Corpus Christi (Figure 12). The underestimation may have resulted from current UAV image processing

technology not being able to identify senesced leaf tissue, although high-resolution sensors were used. In addition, wind also may have affected the accuracy of data collection with the UAV. Although UAV-based maximum plant height tended to slightly overestimate actual plant height, its distribution was closer to ground truth data than UAV-based mean plant height. Thus, using UAV-based maximum plant height may increase accuracy, which is consistent with the Xu's research result (Xu et al., 2019).

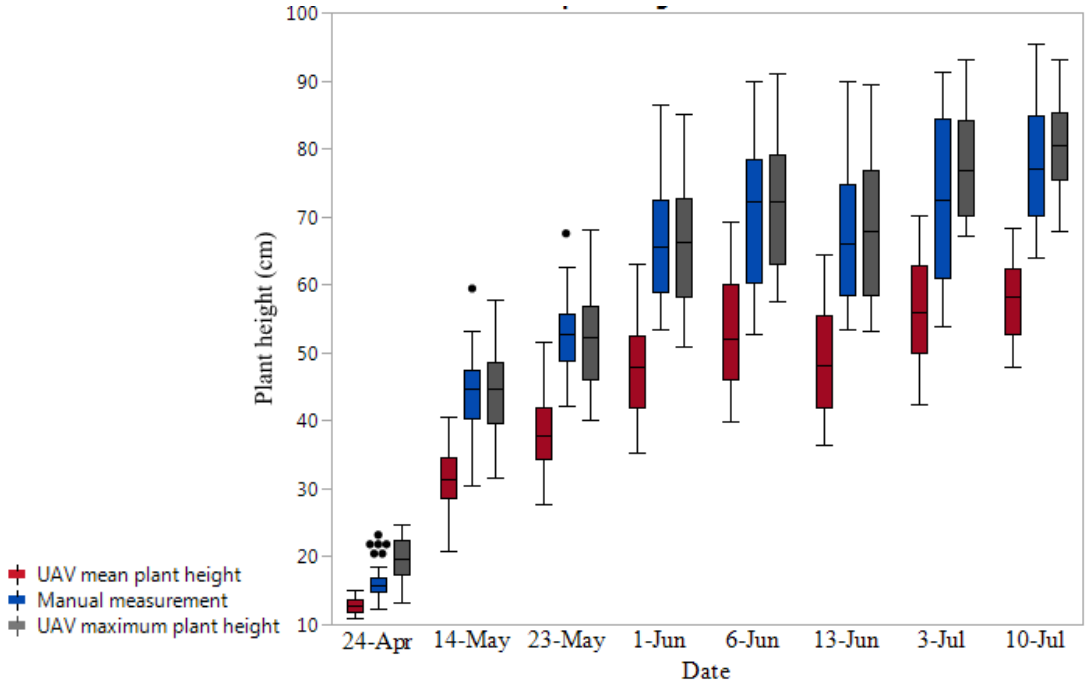

Figure 12. Comparison of UAV-derived mean plant height, manual measurement and UAV-derived maximum plant height at Corpus Christi, TX, in 2018.

4.1.2. Comparison of UAV-derived mean plant height and maximum plant height

Correlations between two types of UAV-based plant height and manual ground measurement were performed. UAV-based maximum plant height was better correlated with ground truth measurement (R^2 0.955) in comparison with UAV-based mean plant height (R^2 0.945) (Figure 13). However, the Root Mean Square Error (RMSE) statistical analysis indicated that maximum plant height had a higher level of error compared to mean plant height. The higher

level of error could be attributed to some plants that are outliers in terms of plant height within a grid especially late in the growing season and windy conditions during data collection. This may not be a problem after maximum plant height achieved because the most practical purpose is to measure plant height during the crop's vegetative and early reproductive stages. Therefore, current UAV-based maximum plant height generally is more accurate and useful when breeders want to predict plant height using UAV before maximum height achieved. Overall, current plant height prediction accuracy is sufficient for cotton phenotyping and management of plant growth regulator application, which is consistent with previous reports in the literature (Sun et al., 2017; Malambo et al., 2018).

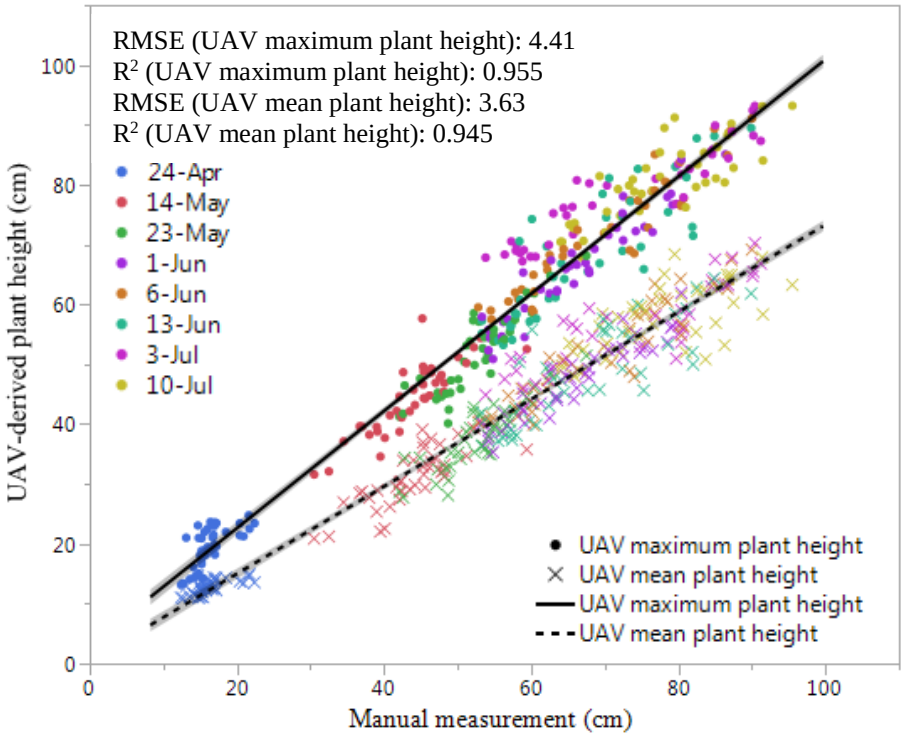

Figure 13. Correlation between UAV-based plant height and manual ground measurements for plant height at Corpus Christi, TX, in 2018.

4.1.3. Comparison of UAV derived maximum plant height from different planting patterns

UAV-based maximum plant height was analyzed independently for the skip-row pattern and the solid-row pattern in order to compare the influence of row width upon the data accuracy using the 3D point cloud. The skip-row planting pattern provided a more accurate plant height (R^2 0.97) with lower levels of error (RMSE 3.92) compared to data collected from the solid-row pattern (R^2 0.93; RMSE 4.70) (Figure 14). Row width may have an impact on the accuracy of PH Model. Biases also potentially resulted from inaccuracies in SfM reconstructions, and in the generation of 3D point clouds. Malambo et al. (2018) found that accuracy of plant height measurements using SfM is not stable during the growing season, which may be influenced by the changes in the plant's leaf reflectance as the plant matures. In summary, skip-row patterns may provide more accurate plant height from PH Model. However, if the ground is flat and there are minimal variations in elevation, we could use the non-planted alleyways between plots as the ground elevation to calculate plant height, possibly diminishing the advantage when using skip-row patterns to predict plant height.

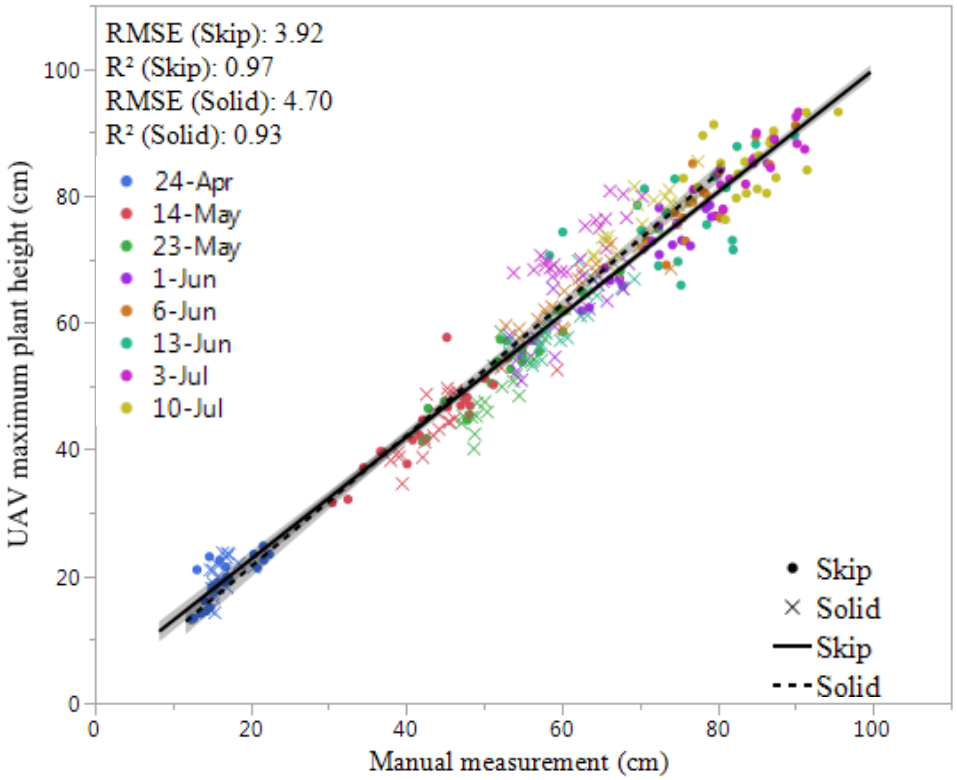

Figure 14. The relationship between UAV based- maximum plant height from different planting patterns and manual ground measurements at Corpus Christi, TX, in 2018.

4.2. UAV yield prediction

4.2.1. Comparison of ground-truth open boll count, UAV-based open boll count and boll area

Open cotton boll counts were randomly measured per meter within each plot on 27 September, and cotton was harvested on 17 November at College Station. In Corpus Christi, the selected meter was randomly chosen within each plot just prior to harvest on 30 July. A UAV flight mission was also performed on the same date as manual measurements. The correlation between manual boll count and UAV-based boll count at Corpus Christi (R^2 0.63) was better than at College Station (R^2 <0.01) (Figure 15). The lack of correlation at College Station may have resulted from the late harvesting. Also, most cotton bolls fell apart due to excessive rain and

wind. On the contrary, open boll count estimates at Corpus Christi were unaffected by extreme weather.

Many factors likely caused the poor correlation between the manual open boll count and the UAV-based boll count. The manual open boll count measurements per plot had errors because they were transferred from open boll count per meter when plants within the same plot were unevenly distributed. Furthermore, measurement effectiveness may be affected by working hours and weather. In regard to UAV-based open boll count, processing technology can only identify open cotton bolls visible in the orthomosaic images but cannot count open bolls below the canopies. Additionally, some cotton boll candidates were wrongly classified since the cotton spectral signature did not have adequate contrast with the background because of shadows, branches and leaves. Another classification error is the bare wet soil, which may be identified as cotton bolls because of the similar spectral signature with open cotton bolls. These factors may result in a poor correlation between UAV-based open boll count and manual measurements.

However, the main purpose of open boll counts is to predict cotton yield. It is obvious that UAV technology did a better job than manual measurement. The correlation between UAV-based open boll count and yield (R^2 0.677; R^2 0.50) was much better than the correlation between manual measurements and yield (R^2 0.52; R^2 0.10) at Corpus Christi and College Station, respectively (Figure 16 and 17). Due to nadir view, cotton bolls on the upper canopy and lower canopy look like they are connected in the orthomosaic images and consequently the algorithm will count them as one boll. The UAV-based open boll area was more predictive of cotton yield (R^2 0.684) at Corpus Christi (Figure 18), which is consistent with Yeom's research results (2018). Yield prediction at College Station was influenced by the extreme weather, which resulted in the underestimation of open cotton boll area because cotton bolls on the lower canopy

were not displayed on orthomosaic images. This effect can be increased by excessive wind and rain, which also contributes to more distortion in orthomosaic images and consequently influence the accuracy of open boll detection. Therefore, UAV-based boll count was more predictive of yield at College Station (R^2 0.50) than UAV-based boll area (R^2 0.41) (Figure 17 and 18).

The primary benefits of UAV remote-sensing technology are to automatically separate cotton bolls from background and directly predict crop yield. Results showed the number of cotton open bolls and open boll area were correlated with the harvested yield. Another benefit is that UAV-based boll count and area only need late-season data. Overall, without extreme weather effect, UAV cotton boll detection is a novel method that enables cotton boll extraction in an automated process, which is efficient for yield prediction ($R^2 > 0.67$).

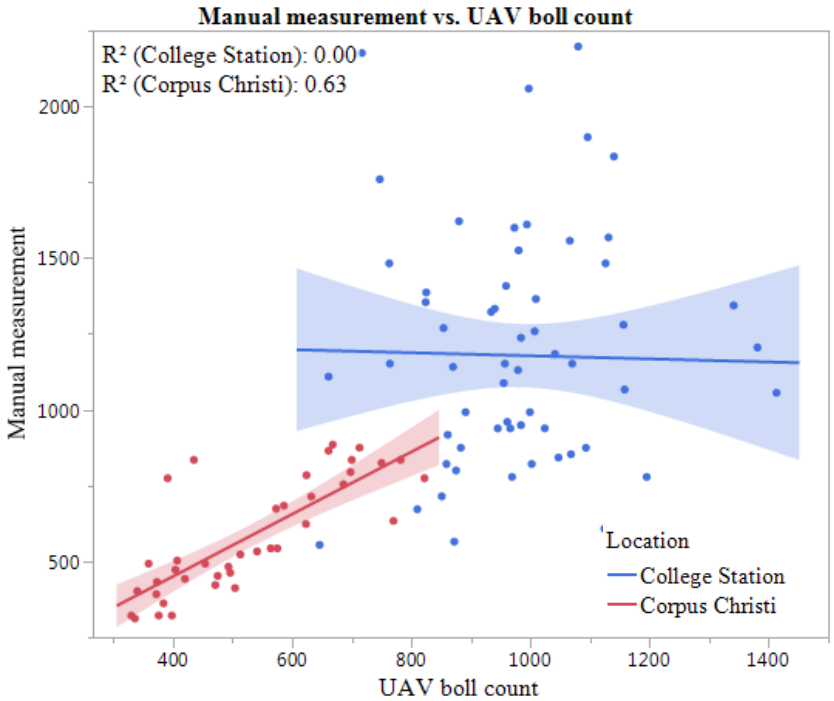

Figure 15. Correlation between manual boll count measurement and UAV-based boll count at Corpus Christi and College Station, TX, in 2018.

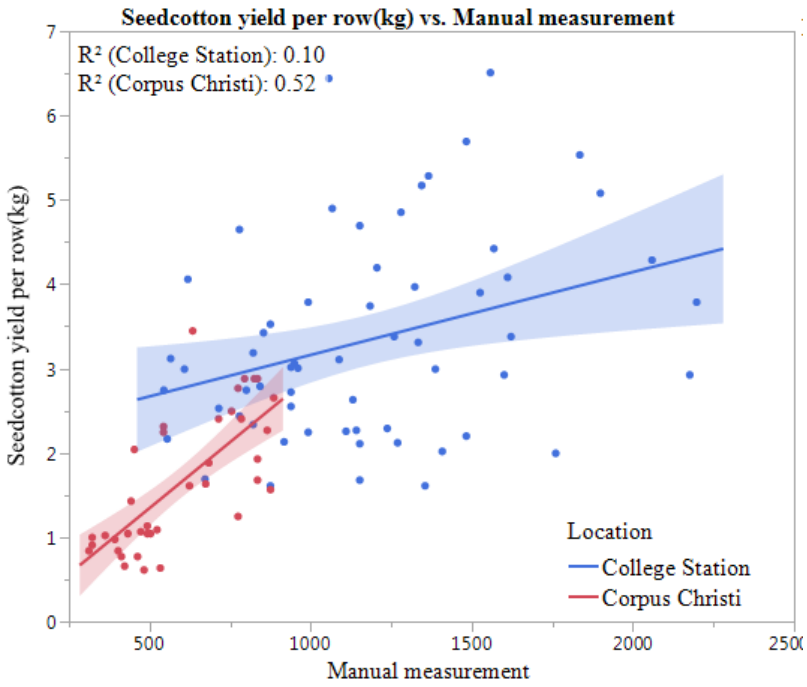

Figure 16. Correlation between manual boll count measurement and yield per row at Corpus Christi and College Station, TX, in 2018.

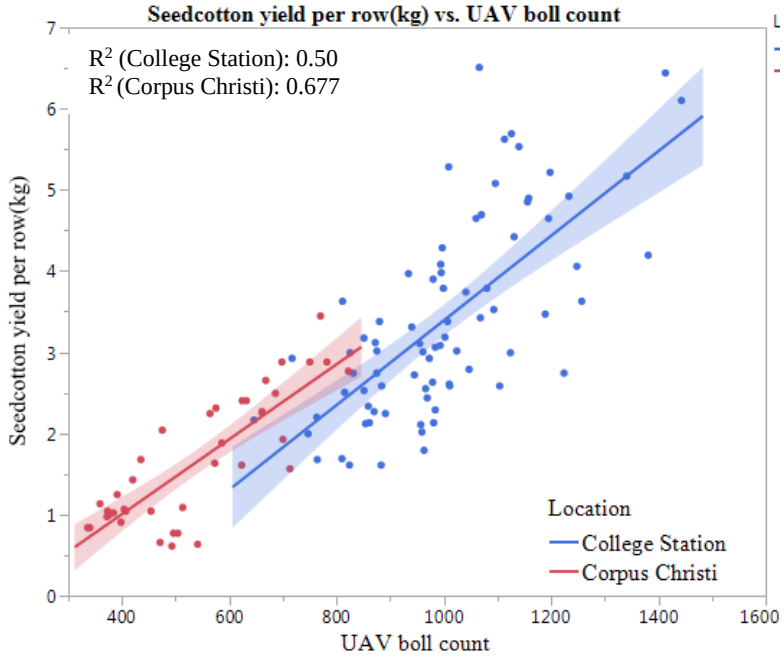

Figure 17. Correlation between UAV-based boll count measurement and yield per row at Corpus Christi and College Station, TX, in 2018.

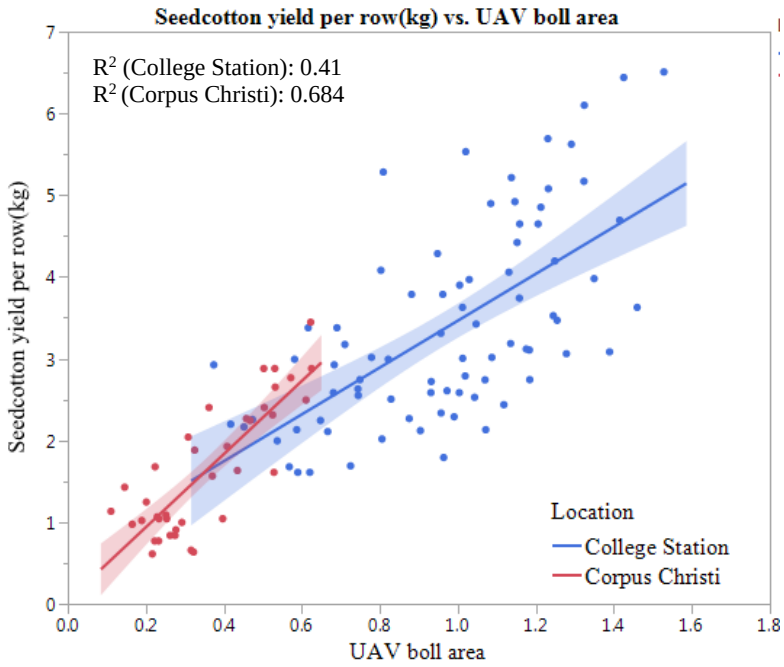

Figure 18. Correlation between UAV-based boll area measurement and yield per row at Corpus Christi and College Station, TX, in 2018.

4.2.2. Comparison of UAV derived open boll count and open boll area from different planting patterns

UAV-based open boll count and open boll area from the skip-row pattern and the solid-row pattern were analyzed separately in order to better compare the influence of row pattern on accuracy. Results showed the skip-row planting pattern had better accuracy in predicting actual harvested yield. The R^2 of the correlations between UAV-based boll count from skip-row pattern and yield were 0.48 and 0.47 while the R^2 of the correlations between UAV-based open boll count from solid-row pattern and yield were 0.28 and 0.1 (Figure 19 and 20) at College Station and Corpus Christi, respectively in 2018. With regards to UAV-based open boll area (Figure 21 and 22), data from the skip-row pattern (R^2 0.64; R^2 0.45) showed better performance in predicting harvested yield than the solid-row pattern (R^2 0.55; R^2 0.25) at College Station and Corpus Christi, respectively. The superiority of UAV data likely resulted from the inability of

sensors to measure lower bolls in the canopy. In summary, the skip-row pattern would provided more accurate UAV-based open boll count and boll area data from orthomosaic images.

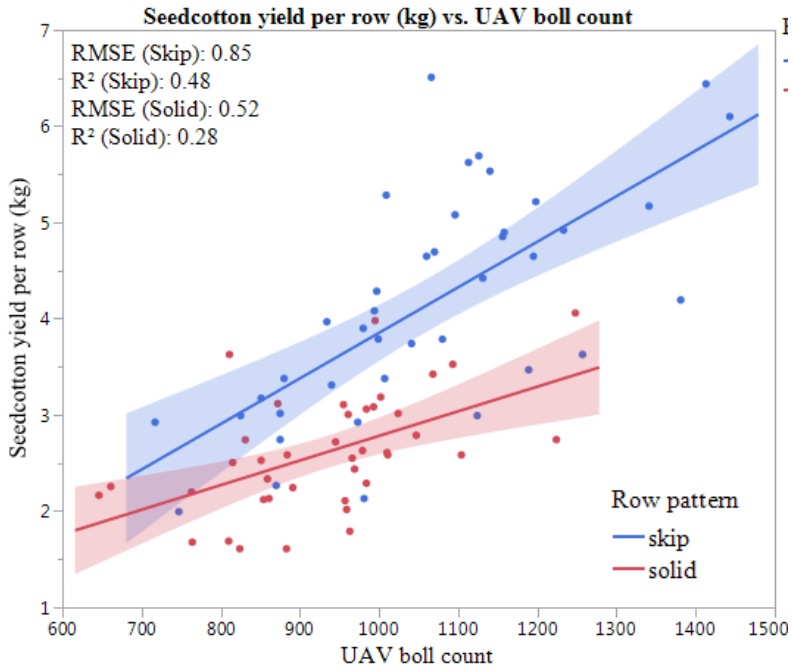

Figure 19. Correlation between UAV based-boll count from different planting patterns and yield per row at College Station, TX, in 2018.

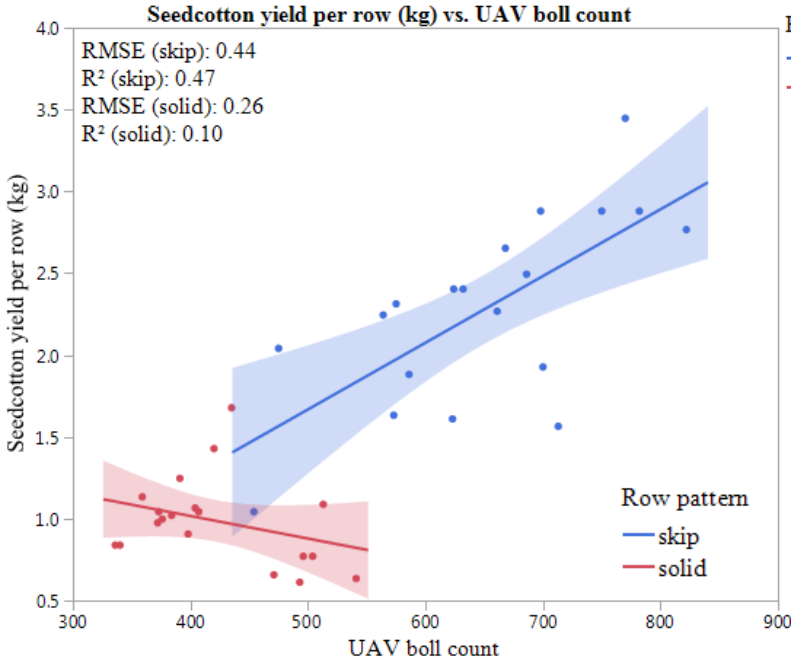

Figure 20. Correlation between UAV based-boll count from different planting patterns and yield per row at Corpus Christi, TX, in 2018.

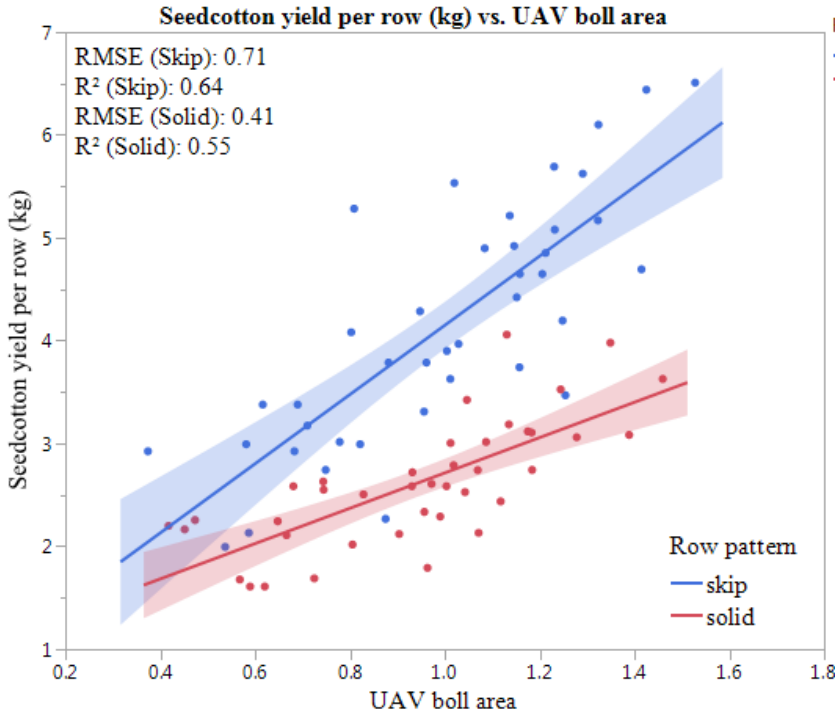

Figure 21. Correlation between UAV based-boll area from different planting patterns and yield per row at College Station, TX, in 2018.

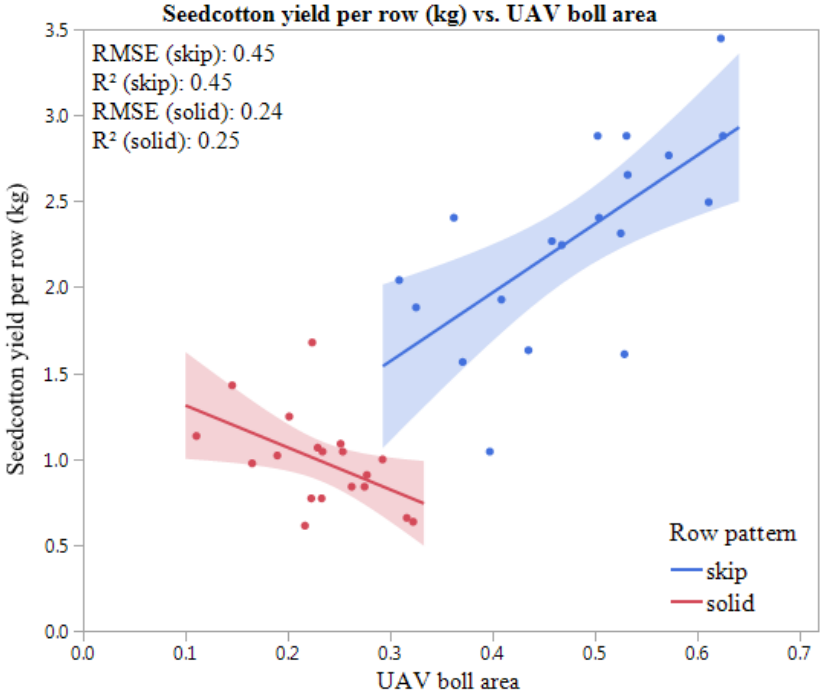

Figure 22. Correlation between UAV based-boll area from different planting patterns and yield per row at Corpus Christi, TX, in 2018.

4.3. UAV parameters' yield predictions comparison

4.3.1. Single parameter yield prediction

There are many alternative ways to estimate cotton yield throughout the growing season. Correlation analysis was performed between the actual lint yield per row (kg) and all the UAV-based data, which includes CC, PH, CV, NDVI, ExG, boll count, and boll area. Because of plant lodging and late harvesting, cotton yield was largely influenced by the environment at College Station (Figure 23 and 24), which probably resulted in the poor correlation between all the UAV-based data and yield at College Station from 12 July to 27 September.

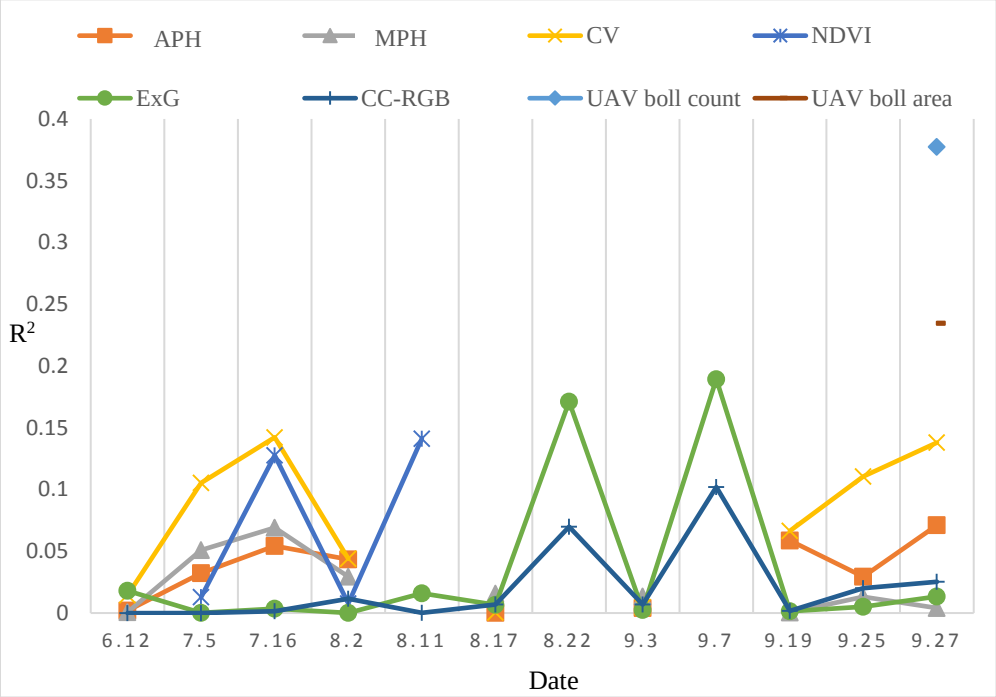

Figure 23. Correlation comparison between UAV data and yield throughout the whole growing season at College Station (Irrigated), TX, in 2018.

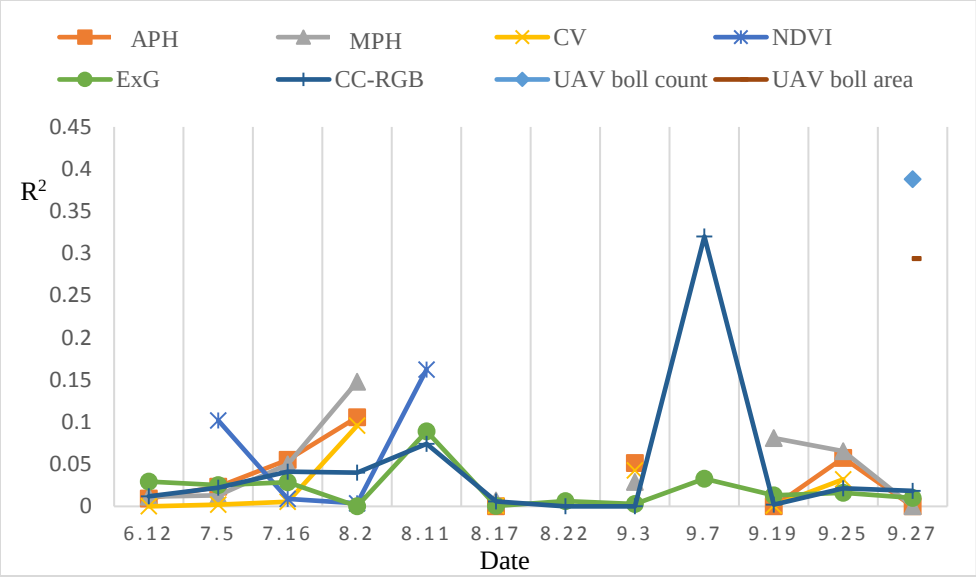

Figure 24. Correlation comparison between UAV data and yield throughout the whole growing season at College Station (dryland), TX, in 2018.

Correlation analysis also was performed from 11 April to 30 July at Corpus Christi in 2018 (Figure 25). There were weak correlations between all the UAV-based data and yield for the data collected from the germination and emergence stage (23 April) to about the 1st Bloom stage (23 May). After this period, yield estimation models using maximum plant height (MPH) and average plant height (APH) have a similar trend. The coefficient of determination of the correlation between yield and MPH dramatically increased to above 0.65 during mid-season from 45 days to 70 days after planting. Then MPH and APH lost the ability to estimate yield after about first open boll stage (09 July) because UAV remote sensing cannot detect the plants' terminal after leaf senescence.

In terms of CV, after 1st Bloom stage (23 May), the coefficient of determination dramatically increased and then stabilized around 0.6 until cotton-harvesting. This result was consistent with Chu et al. (2016), who shows canopy volume is a robust and useful yield predictor in the middle and late season. CC is another trait of interest as it relates to crop growth and development. The coefficient of determination dramatically increased and then stabilized

during mid-season. NDVI-based canopy cover is more predictive of yield since R^2 is almost twice the level of RGB-based R^2, because RGB-based canopy cover may be affected by the change in leaf coloration while NDVI-based canopy cover relies on the red and near-infrared bands, rather than green band. After defoliation, UAV-based canopy covers obviously lost the ability to predict yield.

As for two vegetation indices, the yield correlation trends over the growing season are different because NDVI was generated using multispectral sensors while ExG was processed using RGB sensors. After the poor correlation with lint yield from germination and the emergence stage (23 April) to about 1st Bloom stage (23 May), the coefficient of determination of ExG dramatically increased to 0.58 and then fluctuated during mid-season. Then ExG lost the ability to predict yield after 5 nodes above white flowers (NAWF) stage (13 June), which may possibly be the result of the leaf transition to a more yellow coloration. NDVI has a better correlation with yield than ExG, which is a similar result to Zhou. et al (2017) with rice. After that time period, NDVI was not able to estimate yield due to defoliation (19 July).

In addition, cotton boll count and area were processed just before harvest (30 July). The correlation between UAV-based boll area and yield (R^2 0.684) was slightly better than boll count measurements (R^2 0.677).

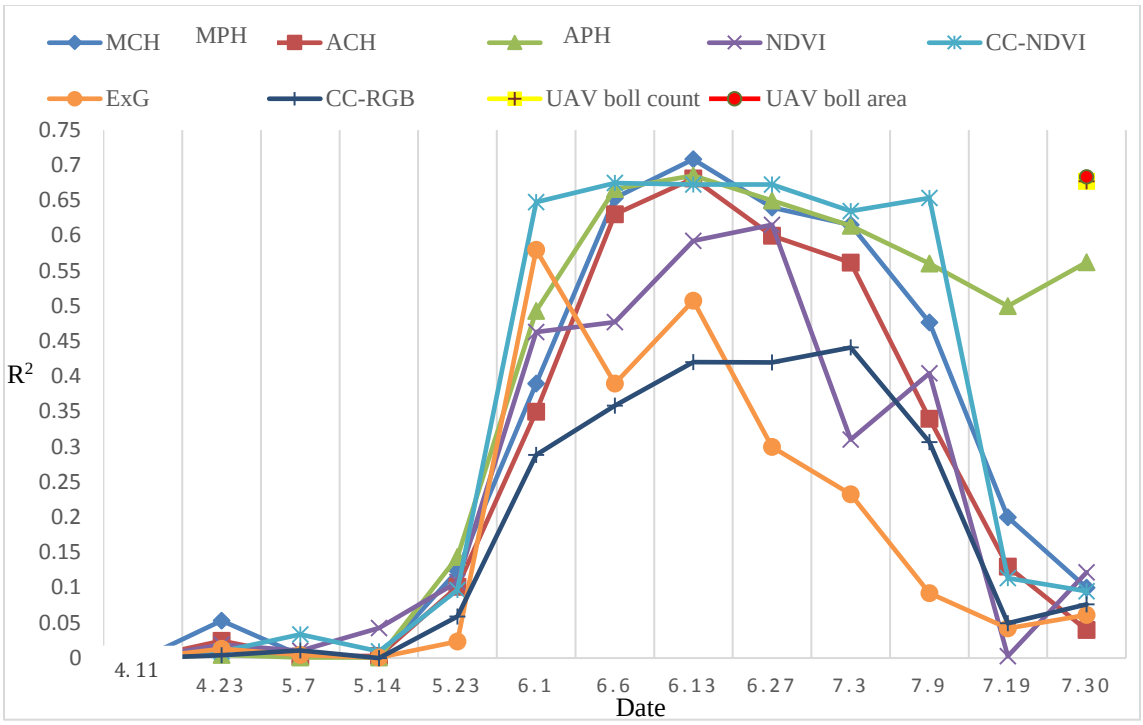

Figure 25. Correlation comparison between UAV data and yield throughout whole growing season at Corpus Christi, TX, in 2018.

Overall, the three most predictive parameters were maximum plant height at 5 NAWF stage (R^2 0.708), CV at 5 NAWF stage (R^2 0.685) and boll area just before harvest (R^2 0.684). This result should help breeders predict yield using a single parameter by flying UAV once at those growing stages mentioned above, saving time and resources for the breeders.

4.3.2. Best yield predictors combination

In order to fully take advantage of UAV data, stepwise regression was used to select appropriate combinations of variables for prediction models and removing unnecessary parameters. All the UAV-based data was fed into the model to find the best yield predictor combinations. The Stopping rule and direction were set as Minimum Bayes information criterion (BIC= -2loglikelihood + p log n) and forward respectively. All the UAV-based data were fed

into the model to find the best predictors combination for lint yield per row (kg) aiming to maximize prediction accuracy.

After running stepwise regression analysis, the first model from the results showed a much better correlation (R^2 0.907) with cotton yield than single predictors. This model included MPH at 4 true leaves stage (23 May), MPH at 5 NAWF stage (13 June), NDVI at germination and emergence stage (23 April), pre-defoliation CC-RGB (19 July), and pre-harvest (30 July) UAV boll count and canopy cover (Table 1). This model is significant (Table 2) but there are two insignificant predictors in this model (Table 3), pre-defoliation CC-RGB (19 July) and pre-harvest canopy cover (30 July). In order to increase efficiency and save time and money, a second model was generated after removing these two insignificant predictors. Results showed the second model with four parameters was significant and the R^2 was 0.863 (Table 4 and Table 5), which is slightly lower than the first model. However, there is a new insignificant predictor appeared in the second model, NDVI at germination and emergence stage (23 April) (Table 6). A third model was created after eliminating the insignificant predictor in the second model. This model was significant and R^2 was 0.854 (Table 7), with three significant parameters (Table 8 and Table 9), MPH at 4 true leaves stage (23 May), MPH at 5 NAWF stage (13 June) and pre-harvest UAV boll count (30 July).

Hence, yield can be accurately predicted by using any of these three models. The first model would provide the most accurate yield prediction, but more UAV flight missions would be required with an RGB sensor and a Multispectral sensor. The third model would save money and time because it only needs one flight using an RGB sensor at the 4 true leaves, 5 NAWF and pre-harvest stages respectively. Breeders can choose yield prediction models based on the research purpose and the availability of time and money.

Table 1. Summary of fit for the first model from stepwise at Corpus Christi, TX, in 2018.

Summary of Fit	
R Square	0.907
R Square Adj	0.889
Root Mean Square Error	0.582
Mean of Response	3.603
Observations (or Sum Wgts)	38

Table 2. Analysis of variance for the first model from stepwise at Corpus Christi, TX, in 2018.

Analysis of Variance				
Source	**DF**	**Sum of Squares**	**Mean Square**	**F Ratio**
Model	6	103.005	17.168	50.639
Error	31	10.509	0.339	**Prob > F**
C. Total	37	113.514		<.0001*

Table 3. Parameter estimates for the first model from stepwise at Corpus Christi, TX, in 2018.

Parameter Estimates				
Term	**Estimate**	**Std Error**	**t Ratio**	**Prob>|t|**
Intercept	-10.877	2.656	-4.09	0.0003*
MPH 5/23	-0.139	0.036	-3.84	0.0006*
MPH 6/13	0.168	0.022	7.64	<.0001*
NDVI 04/23	12.899	5.109	2.52	0.0169*
CC-NDVI 7/30	-0.065	0.069	-0.95	0.3505
CC-RGB 7/19	-0.039	0.023	-1.67	0.1041
UAV boll count 7/30	0.005	0.001	4.69	<.0001*

Table 4. Summary of fit for the second model from stepwise at Corpus Christi, TX, in 2018.

Summary of Fit	
R Square	0.863
R Square Adj	0.847
Root Mean Square Error	0.686
Mean of Response	3.603
Observations (or Sum Wgts)	38

Table 5. Analysis of variance for the second model from stepwise at Corpus Christi, TX, in 2018.

Analysis of Variance				
Source	**DF**	**Sum of Squares**	**Mean Square**	**F Ratio**
Model	4	97.980	24.495	52.036
Error	33	15.534	0.471	**Prob > F**
C. Total	37	113.515		<.0001*

Table 6. Parameter estimates for the second model from stepwise at Corpus Christi, TX, in 2018.

Parameter Estimates				
Term	**Estimate**	**Std Error**	**t Ratio**	**Prob>|t|**
Intercept	-7.742	2.877	-2.69	0.0111*
MPH 5/23	-0.108	0.032	-3.33	0.0022*
MPH 6/13	0.139	0.022	6.47	<.0001*
NDVI 04/23	7.627	5.123	1.49	0.1460
UAV boll count 7/30	0.005	0.001	4	0.0003*

Table 7. Summary of fit for the third model from stepwise at Corpus Christi, TX, in 2018.

Summary of Fit	
R Square	0.854
R Square Adj	0.841
Root Mean Square Error	0.698
Mean of Response	3.603
Observations (or Sum Wgts)	38

Table 8. Analysis of variance for the third model from stepwise at Corpus Christi, TX, in 2018.

Analysis of Variance				
Source	**DF**	**Sum of Squares**	**Mean Square**	**F Ratio**
Model	3	96.937	32.312	66.271
Error	34	16.577	0.487	**Prob > F**
C. Total	37	113.514		<.0001*

Table 9. Parameter estimates for the third model from stepwise at Corpus Christi, TX, in 2018.

Parameter Estimates				
Term	**Estimate**	**Std Error**	**t Ratio**	**Prob>|t|**
Intercept	-3.680	0.928	-3.96	0.0004*
MPH 5/23	-0.075	0.025	-3.09	0.0040*
MPH 6/13	0.127	0.020	6.25	<.0001*
UAV boll count 7/30	0.005	0.002	3.81	0.0006*

4.4. Visual ratings and actual yields comparison

Every single rows were manually rated from 1 to 7 from planting to harvesting. Visual rating for each single row was performed based on orthomosaic images (Figure 26) and 3D point cloud images (Figure 27) of 10 different dates at Corpus Christi and 12 different dates at College Station respectively.

Figure 26. Orthomosaic images in the late season at Corpus Christi, TX, in 2018.

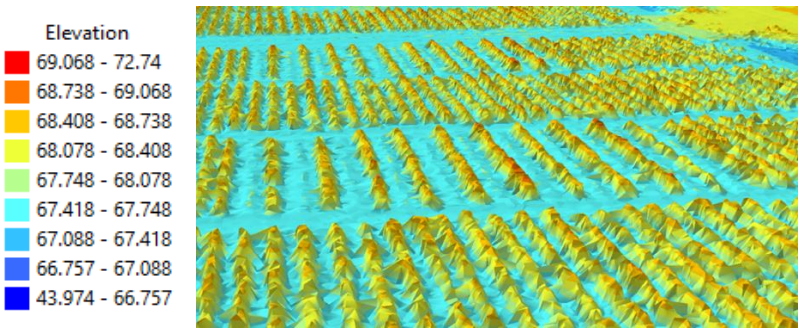

Figure 27. 3D point cloud displayed elevation in the middle season at Corpus Christi, TX, in 2018.

The ranking of five varieties from the solid-row pattern at Corpus Christi showed similarity between the visual rating and the actual yield (Table 10), though the rankings are not identical. For example, Tamcot 211 and Tamcot 73 do not follow this pattern. Tamcot 211 had a higher visual rating than Tamcot 73 but lower actual yield. However, actual yields of these two varieties are not significantly different. Thus, this exception does not negate the overall pattern of similarity. The skip-row pattern's visual rating had a similar result to solid rows (Table 10). TAM X-26-3 had a lower visual rating than Tamcot 73, but the lint yields of these two varieties did not have a significant difference.

In spite of the fact that lodging hampered judgments in scoring yield, visual ratings at College Station irrigated and dryland trials had the same results as Corpus Christi (Table 11 and 12). Moreover, correlations between visual ratings for five varieties and their actual yields were calculated. Visual ratings performed best at Corpus Christi (Figure 28) because cotton at College Station was affected by the extreme weather. Visual ratings from skip-row patterns showed a better correlation than from solid-row pattern (Figure 29) because they are less likely to be affected by canopy closure.

All of these results suggested that visual rating is able to predict cotton yield reasonably well, a conclusion that is consistent with Bowman's research (2004). Breeders can use UAV

images to choose superior progeny rows, which have better yield performance, instead of physically going to the field and making selections. The bird's-eye view images can be acquired periodically to show farmers and breeders crop changes over time. This method is efficient and time-saving.

Table 10. Visual rating and actual yield rankings at Corpus Christi, TX, in 2018.

Corpus Christi 2018						
Genotype	**Row type**	**Average Rating**	**Genotype**	**Row Type**	**Lint yield (kg/ha)**	
Tamcot 421	solid	5.288	Tamcot 421	solid	559.228	A†
Tamcot 211	solid	5.013	Tamcot 73	solid	463.931	AB
Tamcot 73	solid	4.830	Tamcot 211	solid	434.778	AB
TAM X-26-3	solid	4.813	TAM X-26-3	solid	361.831	B
TAM T-08	solid	4.550	TAM T-08	solid	334.680	B
Tamcot 421	skip	5.888	Tamcot 421	skip	624.609	A†
Tamcot 73	skip	5.430	Tamcot 73	skip	603.897	A
Tamcot 211	skip	5.400	TAM X-26-3	skip	466.290	B
TAM X-26-3	skip	4.900	Tamcot 211	skip	417.640	B
TAM T-08	skip	4.338	TAM T-08	skip	399.615	B

†Means followed by the same letter are not different (α=0.05, t-test); means within section are compared.

Table 11. Visual rating and actual yield rankings at College Station (Irrigated), TX, in 2018.

College Station (Irrigated) 2018						
Genotype	**Row type**	**Average Rating**	**Genotype**	**Row Type**	**Lint yield (kg/ha)**	
Tamcot 211	solid	6.042	Tamcot 211	solid	869.298	A†
Tamcot 73	solid	6.042	Tamcot 73	solid	781.983	AB
TAM T-08	solid	5.819	TAM X-26-3	solid	691.788	AB
Tamcot 421	solid	5.667	Tamcot 421	solid	673.855	AB
TAM X-26-3	solid	5.472	TAM T-08	solid	649.678	B
Tamcot 421	skip	6.181	Tamcot 421	skip	888.834	A†
TAM T-08	skip	5.778	TAM T-08	skip	711.280	AB
Tamcot 73	skip	5.514	Tamcot 211	skip	609.675	ABC
Tamcot 211	skip	5.403	Tamcot73	skip	601.706	BC
TAM X-26-3	skip	5.056	TAM X-26-3	skip	493.196	C

†Means followed by the same letter are not different (α=0.05, t-test); means within section are compared.

Table 12. Visual rating and actual yield rankings at College Station (Dryland), TX, in 2018.

College Station (Dryland) 2018						
Genotype	**Row type**	**Average Rating**	**Genotype**	**Row Type**	**Lint yield (lbs/ac)**	
Tamcot 421	solid	6.000	Tamcot 211	solid	1333.228	A†
Tamcot 73	solid	5.882	Tamcot 421	solid	1288.451	A
Tamcot 211	solid	5.706	Tamcot73	solid	1163.117	AB
TAM T-08	solid	5.412	TAM T-08	solid	967.428	BC
TAM X-26-3	solid	5.294	TAM X-26-3	solid	894.618	C
Tamcot421	skip	6.118	Tamcot 421	skip	1063.799	A†
Tamcot 211	skip	6.000	Tamcot 211	skip	941.301	AB
Tamcot 73	skip	5.941	Tamcot 73	skip	800.242	AB
TAM T-08	skip	5.940	TAM X-26-3	skip	690.074	B
TAM X-26-3	skip	4.588	TAM T-08	skip	684.907	B

†Means followed by the same letter are not different (α=0.05, t-test); means within section are compared.

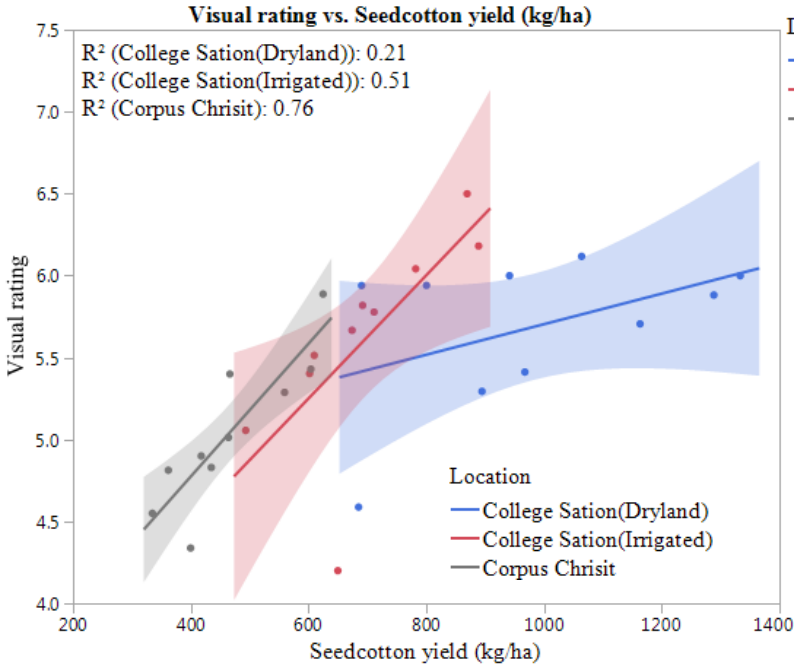

Figure 28. Correlation between visual rating and actual yield at College Station and Corpus Christi, TX, in 2018.

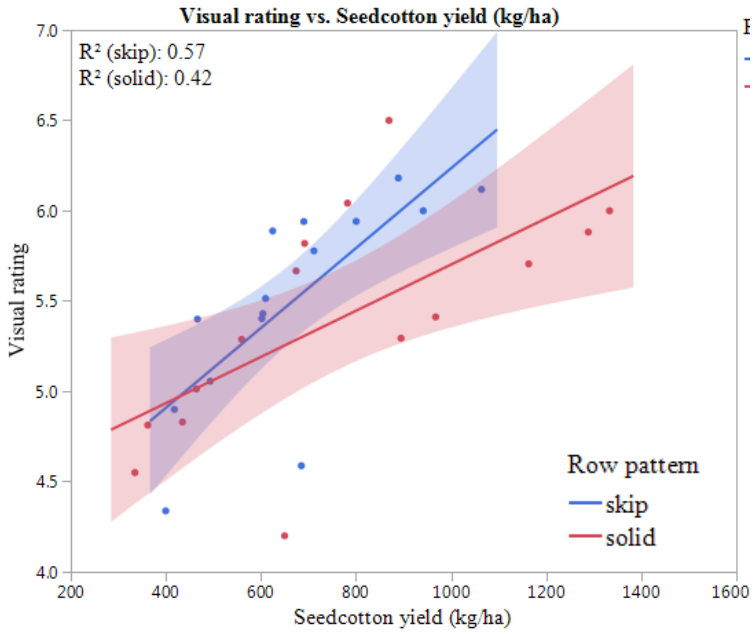

Figure 29. Correlation between visual rating and actual yield from different planting pattern in 2018.

4.5. Genotype x row patterns interaction

4.5.1. Genotype x row pattern interaction at seven individual trials

Analysis of variance was performed to characterize genotype x row pattern interactions and how location and year can affect that interaction using fiber and yield data in 2017 and 2018 from three locations. The analysis of yield data from seven individual trials showed the genotype x row pattern interaction was not significant for lint percent (Table 13). In terms of lint yield, no trial had significant genotype x row pattern interactions except the trial at College Station in 2017. The effects of Hurricane Harvey likely caused this significant interaction for lint yield. In August 2017, about 5.6 cm of rainfall occurred at College Station. Because late maturity in skip-row patterns, those green bolls can still open after the hurricane. However, the lower open bolls in solid-row pattern were damaged due to substantial rainfall leading to row pattern and genotype interaction only being significant for this trial.

The analysis of variance of fiber traits（Table 14) showed the row pattern and genotype interaction was not significant for UHML, strength and uniformity across seven individual trials. The interaction for micronaire was only significant at College Station in 2018, a result that may be attributed to rain delaying cotton harvesting at the end of September and beginning of November in 2018 because rain and late-harvest may have resulted in undesirable micronaire values (Zheng et al., 2012). Also, regrowth may also contribute to lower micronaire values since new bolls will form immature fibers. Additionally, the interaction was not significant for elongation in any trials except in the trial at Weslaco in 2018 partially because there was a flood at Weslaco just a few weeks before we harvest. This result is consistent with a previous research, which found excessive rain has an impact on fiber elongation (Wang et al., 2014).

Overall, genotype by row pattern interactions were minimal under normal conditions at seven individual trials. Breeding progress and fiber traits are likely not affected by row patterns. Most previous studies found the interaction of row width and genotype had little effect on fiber quality except micronaire (Hawkins and Peacock, 1971; Fowler and Ray, 1977). Dong et al. (2006) found lint yield was not significantly influenced by plant density (3.0, 4.5, 6.0 or 7.5 plants/m^2). Thus, the yield and fiber trait response to row pattern by genotype interactions in this study were similar to previous reports.

4.5.2. The effect of year and location on genotype x row pattern interaction

Data from two years and three locations were combined to investigate how location and year affect row pattern by genotype interactions. Except for the dryland trial at College Station in 2018, all the trials were combined to generate a four-way ANOVA table. In terms of lint percent and lint yield, year and location did not affect row pattern x genotype interactions (Table 15). In regard to fiber traits, year and location did not affect row pattern by genotype interactions for

micronaire, UHML, strength and length uniformity (Table 15). As for elongation, there was a significant row pattern x variety x location interaction, meaning that elongation of five different varieties' responses to row pattern depended upon location, but the elongation ranking for five varieties did not change across three locations (Figure 30). Thus, progeny row selection should not be affected by this three-way interaction. In summary, location and year are not likely to influence the genotype by row pattern interaction for fiber yield and quality.

There are some other interesting 3-way interactions. The significant interaction of Genotype x Year x Location for lint yield indicates that the response of five genotypes to row patterns depended upon environmental conditions. Since row patterns did not have significant effect on lint yield, lint yield was averaged across row pattern treatments to better investigate the Genotype x Year x Location interaction (Figure 31). For example, Tamcot 73 had a lint yield increase of 657.67 kg ha^{-1} when location changed from College Station to Weslaco in 2017, but only a 493.90 kg ha^{-1} increase in 2018. Lint yield was influenced by environmental factors, which is consistent with the research of Graybill et al. (1991). In addition, UHML was significantly affected by the genotype x year x location interaction (Figure 32), which was similar to the results reported by Hearn (1976) who found environmental factors such as water deficiency and high temperature impacted fiber length.

Table 13. Analysis of variance of yield components at 7 trials. (Row pattern x genotype interaction).

Yield component	SOV	DF	Mean Square						
			College Station dryland 2018	Corpus Christi 2018	Weslaco 2018	College Station Irrigated 2018	College Station 2017	Corpus Christi 2017	Weslaco 2017
Lint percent	Rep	3	28.39	4.17	0.41	28.34	0.35	0.51	0.76
	Row	1	81.29*	0.11	6.98*	83.22*	3.14	7.94	4.32**
	Rep*Row	3	7.78	7.50	0.52	7.73	0.81	0.51	0.00
	Genotype	4	28.89	22.93***	26.63**	28.85	15.08***	3.00	3.08**
	Genotype*Row	4	14.08	1.60	2.45	14.80	0.77	0.50	0.27
	Residual	24	14.19	3.44	4.08	13.60	0.84	0.87	0.23
Lint yield	Rep	3	37,864.58	10454.58	19,435.72	36594.89	5216.63	2117.40	26499.63
	Row	1	60,923.97	28007.84	765588.82*	196792.09	2662044.03***	2250553.60***	7732564.23***
	Rep*Row	3	13,584.33	4565.18	29719.37	24080.48	2396.83	2841.53	6392.43
	Genotype	4	203,375.11***	41462.14**	428159.96**	25034.32	478976.44***	35528.90*	213032.44***
	Genotype*Row	4	15,829.26	3,977.78	91632.49	35032.90	195680.21***	11348.73	21421.04
	Residual	24	9,828.01	7,408.27	67182.13	20632.68	16862.48	12676.36	27084.67

*, ** and *** represent significant difference at 0.05, 0.01 and 0.001, respectively, and NS represent no significant difference.

Table 14. Analysis of variance of fiber traits at 7 trials. (Row pattern x genotype interaction).

Fiber traits	SOV	DF	Mean Square						
			College Station dryland 2018	Corpus Christi 2018	Weslaco 2018	College Station Irrigated 2018	College Station 2017	Corpus Christi 2017	Weslaco 2017
MIC	Rep	3	0.0276	0.021	0.1794	0.0295	0.115	0.2205	0.0125
	Row	1	0.1004*	0.0014	0.1232	0.1081*	0.016	0.0125	0.5445
	Rep*Row	3	0.0069	0.07*	0.0211	0.0062	0.1473	0.0245	0.1125
	Genotype	4	1.3683***	1.4261***	2.7419***	1.4749***	1.6460***	0.5535**	0.4808*
	Genotype *Row	4	0.0767*	0.0313	0.1245	0.0756*	0.1035	0.0725	0.0445
	Residual	24	0.0257	0.024	0.0681	0.0681	0.0695	0.0725	0.1075
UHML	Rep	3	0.0008	0.0058**	0.0028*	0.0005	0.0199***	0.0186**	0.0001
	Row	1	0.0042*	0.0189***	0.0023	0.0093	0.0006	0.0006	0.0005
	Rep*Row	3	0.0004	0.0001	0.0008	0.0019	0.0032	0.0018	0.0007
	Genotype	4	0.0696***	0.0503***	0.0863***	0.0676***	0.0415***	0.0436***	0.0251**
	Genotype *Row	4	0.0009	0.0019	0.0003	0.0005	0.0008	0.0008	0.0011
	Residual	24	0.0006	0.0011	0.0006	0.0006	0.0022	0.0011	0.0022
Uniformity	Rep	3	0.7843	1.7496	2.7069**	2.0869	15.642***	11.858	0.1445
	Row	1	8.2436*	19.7403	1.56025*	12.8822*	0.144	1.458	1.6245
	Rep*Row	3	0.3238	2.1589*	0.1423	1.1883	0.6367	2.45	0.6125
	Genotype	4	2.0621*	11.5285***	10.5765***	5.1246**	5.3903*	7.9968	4.497
	Genotype *Row	4	1.6438	0.4553	0.3465	0.5741	0.9428	0.2193	1.317
	Residual	24	0.7024	0.6232	0.4908	0.7882	1.6352	2.4365	2.361

Table 14. Continued

Fiber traits	SOV	DF	Mean Square						
			College Station dryland 2018	Corpus Christi 2018	Weslaco 2018	College Station Irrigated 2018	College Station 2017	Corpus Christi 2017	Weslaco 2017
Strength	Rep	3	0.4284	0.5153	1.0413	0.703	28.6523***	10.082*	0.6125
	Row	1	11.3796	0.016	4.356	13.456	0.0723	5.408	0.0605
	Rep*Row	3	2.3531	0.942	0.652	2.0927	2.0469	7.938*	0.4805
	Genotype	4	37.0892***	60.4484***	50.7665***	33.4859***	50.8946***	46.0858***	25.6970***
	Genotype *Row	4	0.8519	1.6816	1.546	1.3704	0.5604	1.9868	1.9705
	Residual	24	0.9435	1.7378	1.6829	1.3335	2.655	1.3138	1.1803
Elongation	Rep	3	0.1782	0.4889	0.4509*	0.35*	0.0887	0.5445	0.008
	Row	1	1.365	1.19025*	0.0023	0.361	0.049	0.0845	1.568
	Rep*Row	3	0.2279	0.0749	0.0656	0.291	0.1697	0.0845	0.128
	Genotype	4	2.3213***	4.9185***	3.6915***	2.9016***	2.629***	2.0193***	0.9955
	Genotype *Row	4	0.1919	0.1003	0.3710*	0.2879	0.2015	0.1483	0.598
	Residual	24	0.235	0.2075	0.1158	0.1101	0.3021	0.1333	0.3318

*, ** and *** represent significant difference at 0.05, 0.01 and 0.001, respectively, and NS represent no significant difference.

Table 15. Significance of main effects and their interaction in analysis of variance of yield components and fiber traits.

SOV	DF	Mean square						
		Lint percent	Lint yield(kg/ha)	MIC	UHML	Uniformity	Strength	Elongation
Year	1	161.66***	13,458,508.21***	0.0344	0.1073**	117.7829**	71.0587**	8.5299**
Location	2	138.03	13,904,890.16**	5.2542	0.0787	13.0299	2.2960	11.6901
Year*Location	2	38.59**	461,743.26***	5.4350***	0.1231***	27.2201*	26.8092	5.1424**
Rep (Year*Location)	18	5.69	33,635.46	0.0906	0.0075***	5.6113***	7.3878***	0.3349
Row	1	24.65	12,110,872.16	0.2026	0.0133	22.0777	9.8870	1.6577*
Year*Row	1	19.10*	3,586,086.24***	0.2054	0.0075*	3.8435	0.8089	0.0027
Location*Row	2	29.79	1,607,140.08	0.0137	0.0013	1.0341	0.0864	0.2238
Year*Location*Row	2	7.32	53,281.11	0.2631*	0.0012	1.5426	5.4714	0.7394*
Rep*Row (Year*Location)	18	2.82	17,919.49	0.0628	0.0015	1.1029	1.8299	0.1440
Genotype	4	74.37*	794,579.21*	6.2409***	0.2771***	34.2105***	241.7301**	13.3946*
Year*Genotype	4	7.40	94,055.29	0.1031	0.0023	0.1481	3.9826	0.3775
Location*Genotype	8	6.52	195,654.52	0.0960	0.0014	3.5743**	3.0831	0.3035
Year*Location*Genotype	8	5.42	160,393.18***	0.2090***	0.0034*	1.3541	1.0661	0.3639
Row*Genotype	4	4.27	83,405.99	0.1024*	0.0031*	0.2323	0.5626	0.8924
Year*Row*Genotype	4	6.67	107,929.86	0.0120	0.0003	0.6013	1.6168	0.2410
Location*Row*Genotype	8	2.60	78,632.19	0.0509	0.0004	0.8853	1.8598	0.6698*
Year*Location*Row*Genotype	8	2.51	77,024.70	0.1004	0.0006	0.7356	1.8473	0.0928
Residual	144	3.78	38,705.88	0.0528	0.0012	1.1007	1.7658	0.1908

*, ** and *** represent significant difference at 0.05, 0.01 and 0.001, respectively, and NS represent no significant difference

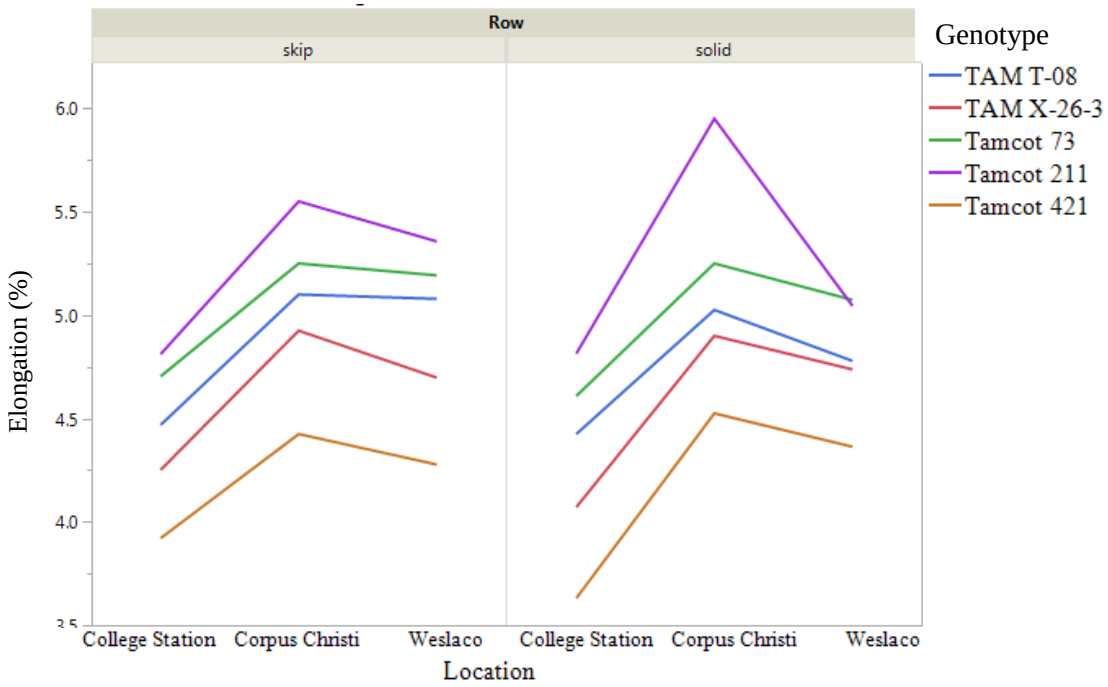

Figure 30. Least Squares Means for fiber elongation of five varieties at three locations in skip-row and solid-row patterns.

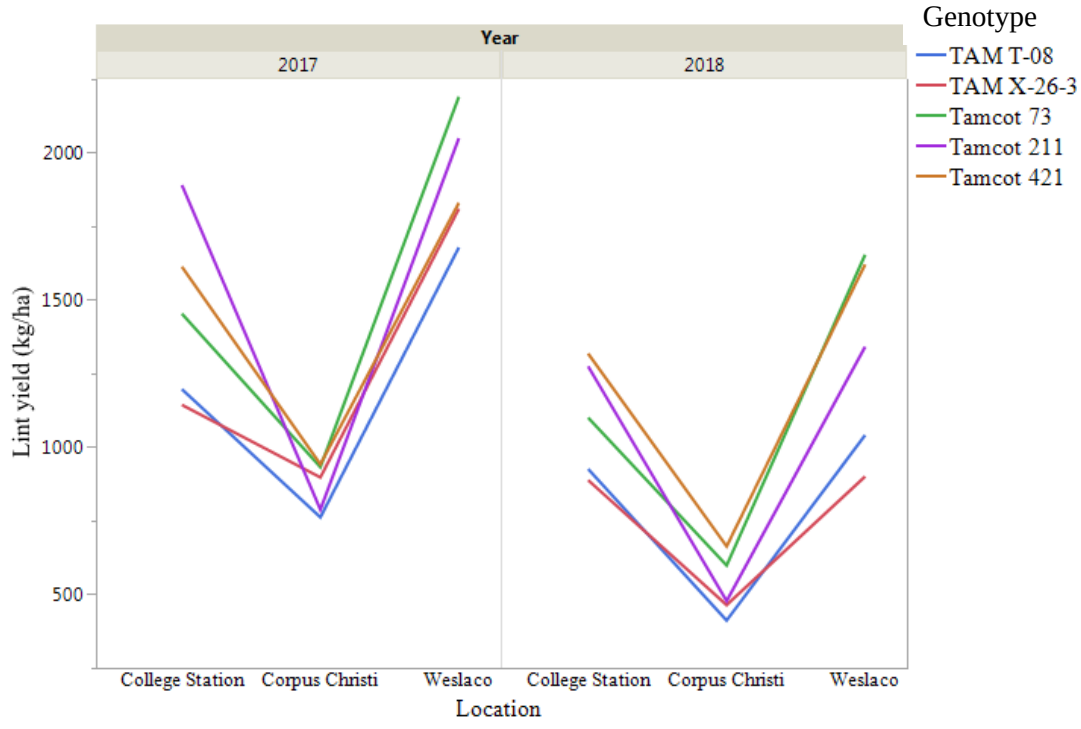

Figure 31. Least Squares Means of Lint yield of five varieties at three locations in 2017 and 2018.

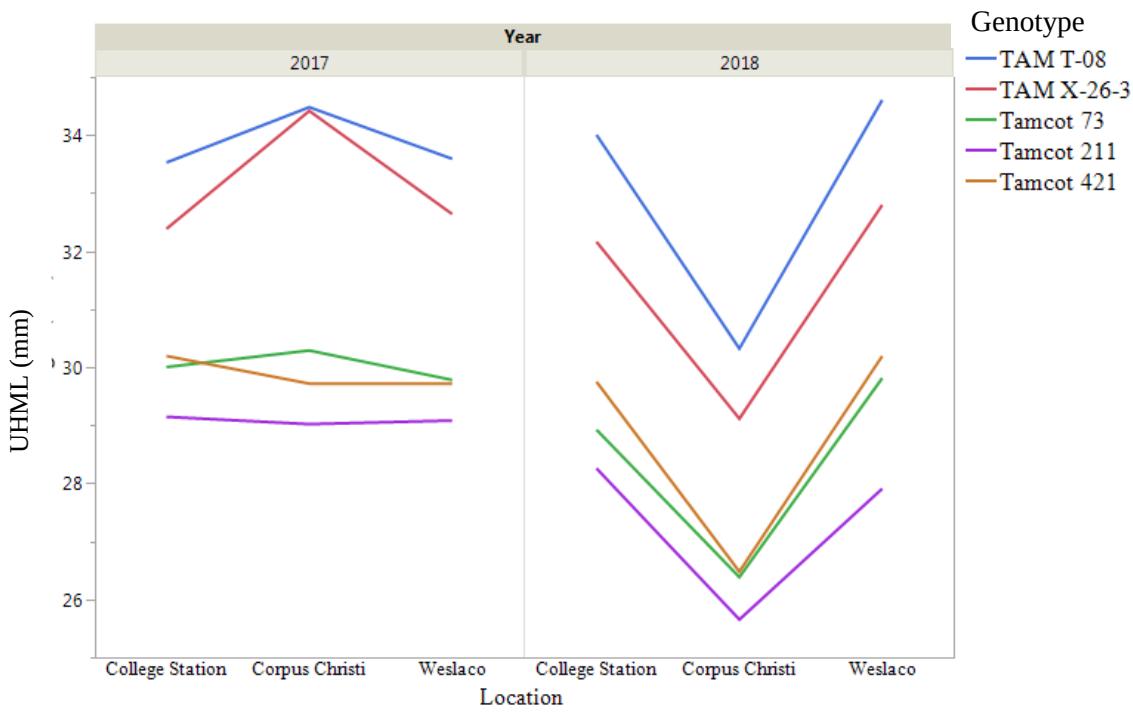

Figure 32. Least Squares Means of UHML of five varieties at three locations in 2017 and 2018.

4.6 GGE biplot of least squares means of lint yield at seven individual trials

We used least squares means of lint yield (kg/ha) at seven individual locations (Table 16) to generate a scatter plot and a ranking biplot, which can help breeders to compare multiple genotypes in multiple environments. Tamcot 73 planted in solid-row pattern had the highest mean yield, followed by solid-row Tamcot 211 (Figure 33). Cotton planted in solid-row patterns had higher yields (kg/ha) than grand mean whereas the skip-row pattern had lower yields (kg/ha) than grand mean. This result is consistent with previous research, which found lint yields (kg/ha) were 13 to 15% lower in skip-row patterns than in solid row patterns (Gwathmey et al., 2008). In addition, the yield of Tamcot 421 from the solid row pattern was highly unstable whereas skip-row pattern Tamcot 421 was highly stable (Figure 33). This finding was consistent with previous reports in the literature, which found lint yield stability would be influenced by population

densities (Bednarz et al., 2005) and the changing environmental conditions (Baloch et al., 2015) because decreased population density resulted in greater fruiting site production and fruit retention (Bednarz et al., 2000). The yield performance of solid-row Tamcot 421 was the best at Weslaco in 2018, at College Station in 2017 and 2018, whereas solid-row Tamcot 73 and solid-row TAMCOT 211 were the best at College Station in 2017. Also, skip-row Tamcot 421 had the best yield performance at Corpus Christi in 2018 (Figure 34).

Table 16. Seven environments information.

Environment	Location	Year	Irrigation status
ENV1	Corpus Christi	2018	Dryland
ENV2	Corpus Christi	2017	Dryland
ENV3	Weslaco	2018	Irrigated
ENV4	Weslaco	2017	Irrigated
ENV5	College Station	2018	Irrigated
ENV6	College Station	2017	Irrigated
ENV7	College Station	2018	Dryland

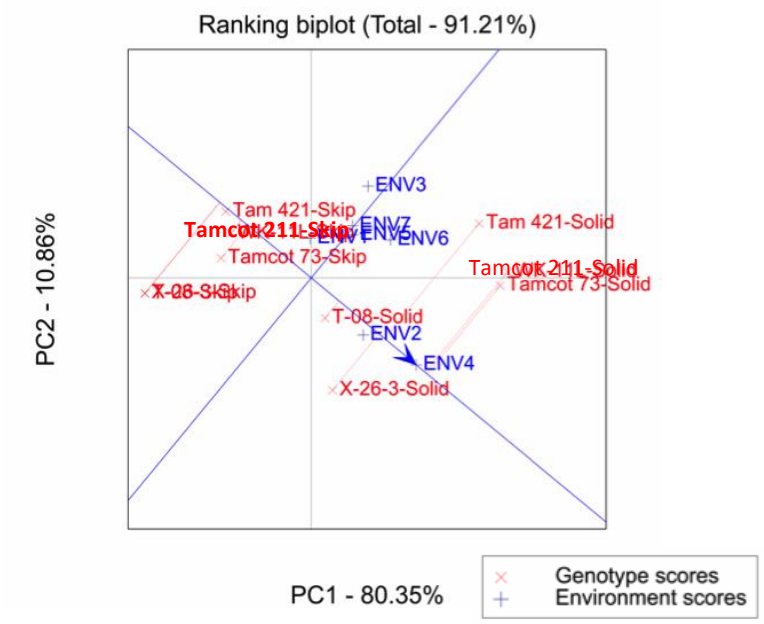

Figure 33. The average-environment coordination view to show the mean performance and stability of the genotype.

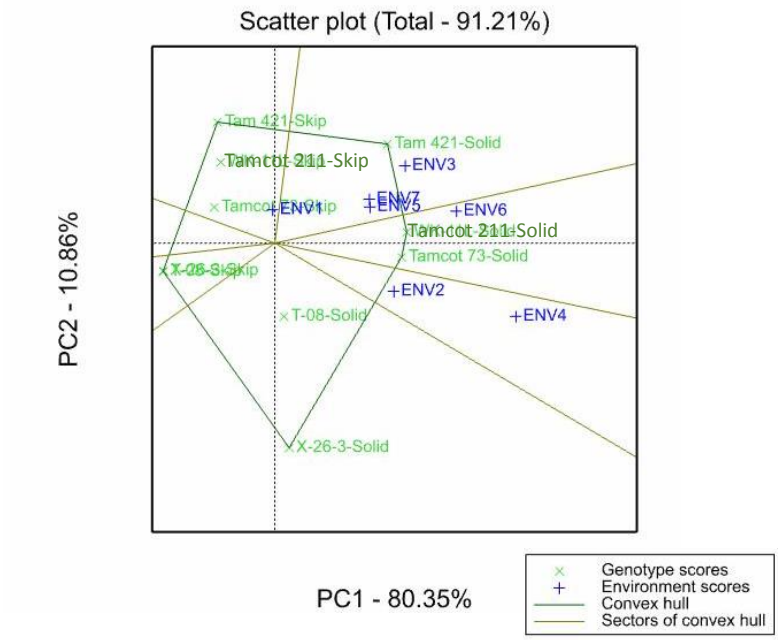

Figure 34. The which-won-where view of the GGE biplot.

5. CONCLUSION

This project had four objectives: (1) use UAVs to characterize genotype x row pattern interaction and how location and year affect that interaction, (2) evaluate the ability of UAVs to predict plant height and yield, (3) compare the accuracy of UAV-derived data from different planting patterns and (4) use images processed from UAVs to standardize data for every single row to predict yield performance. In terms of the first objective, under normal conditions the row pattern by genotype interactions are minimal. Moreover, cotton yield performance and fiber quality are not affected by these interactions, which are not likely to be influenced by year and location.

With respect to the second and third objectives, UAV plant height prediction accuracy is sufficient for cotton phenotyping and management of plant growth (R^2 >0.94). Plant height predictions from skip-row patterns were more accurate than from solid-row patterns. However, if the ground is flat and there are minimal variations in elevation, we could use the non-planted alleyways between plots as the ground elevation to calculate plant height, which may diminish the advantage when using skip-row patterns. In regards to cotton boll detection, UAV remote sensing is a novel way to estimate the number of cotton bolls, which is efficient for yield prediction (R^2>0.65). UAV-derived open cotton boll area and UAV-derived open boll count had better correlation with actual yield than ground-truth boll count. The challenge for this method is that canopy closure prevents the sensor from measuring plant architecture and boll-loads three dimensionally from the mid-growing season until the crop is defoliated. Our results showed UAV-based boll count and boll area generated from skip-row patterns are more predictive of yield than from solid-row patterns. Furthermore, the three most predictive parameters are maximum plant height at 5 NAWF stage (R^2 0.708),

canopy volume at 5 NAWF stage (R^2 0.685) and boll area just before harvest (R^2 0.684). The best yield prediction combination models were generated to maximize yield prediction accuracy (R^2> 0.85). Breeders can choose models based on the research purpose and the availability of their time and money.

The last objective is to standardize data using UAVs for single-row progeny to predict yield performance. The ranking of visual ratings and actual yields are similar, which provides a novel way for breeders to make progeny-row selections. Visual inspection performed better at Corpus Christi because cotton at College Station was affected by extreme weather. Furthermore, visual ratings from skip-row patterns showed better correlation than from solid-row patterns at both locations because they are less likely to be affected by canopy closure.

In summary, yield and plant height estimations were improved when cotton was planted in skip-row patterns. Also, genotype X row-spacing effects are unlikely to change the progeny evaluation decision-making process. Therefore, to take full advantage of UAV data, cotton breeding programs need to plant early generation lines (progeny rows) in skip rows that allow sensors to have access to the view of the ground and capture more accurate 3D images. This can be done without compromising the efficiency and accuracy of the breeding program.

REFERENCES

Azhar, F.M., A.I. Khan, and I. Mahmoud. 1999. Path coefficient analysis of some advanced progenies of G. hirsutum L. Int.J. Agri. Biol. 1(3): 85- 87.

Baloch, M., W. Baloch, M.K. Baloch., A. Mallano., M. Baloch., N.J. Baloch, and S. Abro. 2015. Association and heritability analysis for yield and fibre traits in promising genotypes of cotton (*Gossypium hirsutum L.).* Sindh Univ. Res. J. l 47:303-306.

Bange, M.P., R.L Long, G.A. Constable, and S.G. Gordon, 2010. Minimizing immature fiber and neps in upland cotton. Agronomy Journal. 102:781–789.

Bednarz, C.W., D.C. Bridges, and S.M. Brown. 2000. Analysis of Cotton Yield Stability Across Population Densities. Agronomy Journal 92(1): 128.

Bednarz, C.W., W.D Shurley, W.S Anthony, and R.L Nichols. 2005. Yield, quality, and profitability of cotton produced at varying plant densities. Agronomy Journal, 97:235-240.

Bednarz, C.W., W.D. Shurley, and W.S. Anthony. 2004. Losses in yield, quality, and profitability of cotton from improper harvest timing. Agronomy Journal 94(5):1004-1011.

Bernardo, R., 2003. On the effectiveness of early generation selection in self-pollinated crops. Crop Sci 43:1558–1560.

Berni, J. A. J., P. J Zarco-Tejada, L. Sua´rez, and E. Fereres. 2009. Thermal and narrowband multispectral remote sensing for vegetation monitoring from an unmanned aerial vehicle. IEEE Transactions on Geoscience and Remote Sensing 47(3): 722–738.

Bourland, F. M., D. M. Oosterhuis, and N. P. Tugwell. 1992. Concept for monitoring the growth and development of cotton plants using main-stem node counts. Journal of Production Agriculture 5: 532–538.

Bourland, F. M., N. R. Benson, E. D. Vories, N. P. Tugwell, and D.M. Danforth, 2001. Measuring maturity of cotton of using nodes above white flower. Journal of Cotton Science 5:1–8.

Bowman, D. T, F. M. Bourland, G. O. Meyers, T. P. Wallace, and D. Caldwell. 2004. Visual selection for yield in cotton breeding programs. Journal of Cotton Science 8:26–68.

Byth, D.E., C.R. Weber, and B.E. Caldwell. 1969. Correlated truncation selection for yield in soybean. Crop Science 9:699-702.

Campbell J. B., H. Randolph Wynne. 2011. Introduction to remote sensing. Published by Guilford Press, New York, USA.

Campbell, B.T., and M.A. Jones. 2005. Assessment of genotype × environment interactions for yield and fiber quality in cotton performance trials. Euphytica 144:69–78.

Chang, A., Jung, J., Maeda, M.M., et al., 2017. Crop height monitoring with digital imagery from unmanned aerial system (UAS). Computers and Electronics in Agriculture 141: 232–237.

Chen, R., T. Chu, J.A. Landivar, C. Yang, and M.M. Maeda. 2017. Monitoring Cotton (*Gossypium hirsutum L.)* Germination using Ultrahigh-Resolution UAS Images. Precision Agriculture 1–17.

Chu, T., R. Chen, J. A. Landivar, M. M. Maeda, C. Yang, and M. J. Starek. 2016. Cotton growth modeling and assessment using unmanned aircraft system visual-band imagery. Journal of Applied Remote Sensing, 10(3), 036018.

Colomina, I., and P. Molina. 2014. Unmanned aerial systems for photogrammetry and remote sensing: a review. ISPRS Journal of Photogrammetry and Remote Sensing 92: 79–97.

Constable, G.A., and M.P Bange. 2007. Producing and preserving fiber quality: from the seed to the bale. In: World Cotton Research Conference—4, Lubbock, TX, 10–14 September 2007. International Cotton Advisory Committee/Omnipress.

Dong, H., W. Li, W. Tang, D. Zhang, and Z. Li. 2006. Yield, quality and leaf senescence of cotton grown at varying planting dates and plant densities in the Yellow River Valley of China. Field Crops Research 98: 106–115.

Fang, L., Q. Wang, and Y. Hu. 2017. Genomic analyses in cotton identify signatures of selection and loci associated with fiber quality and yield traits. Nature Genetics 49: 1089–1098.

Farooq, J., M. Anwar, M. Riaz, A. Mahmood, A. Farooq, M.S. Iqbal and M.S Iqbal. 2013. Association and path analysis of earliness in yield and fiber related traits under cotton leaf curl virus (CLCuV) intensive condition in cotton. Plant Knowledge Journal. 2(1):43-50.

Geesing, D., M. Diacono, and U. Schmidhalter. 2014. Site-specific effects of variable water supply and nitrogen fertilisation on winter wheat. Journal of Plant Nutrition and Soil Science 177: 509–523.

Gevaert, C. M., J. Suomalainen, J. Tang, and L. Kooistra. 2015. Generation of spectral–temporal response surfaces by combining multispectral satellite and hyperspectral UAV imagery for precision agriculture applications. IEEE Journal of Selected Topics in Applied Earth Observations and Remote Sensing 8(6): 3140–3146.

Graybill, J.S., W.J. Cox, and D.J. Otis. 1991. Yield and quality of forage maize as influenced by hybrid, planting date, and plant density. Agronomy Journal 83:559–564.

Gutiérrez-Peña, P. A., F. López-Granados, J. M. Peña-Barragán, M. Jurado-Expósito, and C. Hervás-Martínez. 2008. Logistic regression product-unit neural networks for mapping Ridolfia segetum infestations in sunflower crop using multitemporal remote sensed data. Computers and Electronics in Agriculture 64: 293– 306.

Gwathmey, C. O., L. E. Steckel, and J. A. Larson. 2008. Solid and Skip-Row Spacings for Irrigated and Nonirrigated Upland Cotton. Agronomy Journal 100:672-680. doi:10.2134/agronj2007.0240

Hazeem, M. A. B. 2005. Path coefficient analysis in upland cotton. Mesopotamia Journal Agriculture 33: 3.

He D. H., Z. X. Lin, X. L Zhang, Y. C Nie, X. P. Guo, C. D. Feng, J. M. Stewart. 2005. Mapping QTLs of traits contributing to yield and analysis of genetic effects in tetraploid cotton. Euphytica 144:141–149.

Hearn, A.B. 1976. Response of cotton to nitrogen and water in a tropical environment. III. Fibre quality. Journal of Agricultural Science 86(2): 257—269.

Honkavaara, E., H. Saari, J. Kaivosoja, I. Po¨lo¨nen, T. Hakala, and P. Litkey. 2013. Processing and assessment of spectrometric, stereoscopic imagery collected using

a lightweight UAV spectral camera for precision agriculture. Remote Sensing, 5(10): 5006–5039.

Jones, M. A. 1997. Response of cotton growth and development to row spacings and planting patterns, p. 1488. In Proceedings of the Beltwide Cotton Conferences.

Jones, M. A., and R. Wells. 1998. Fiber yield and quality of cotton grown at two divergent population densities. Crop Science 38: 1190–1195.

Jost, P. H., and J. T. Cothren. 2001. Phenotypic alterations and crop maturity differences in ultra-narrow row and conventionally spaced cotton. Crop Sci. 41: 1150–1159.

Jung, J., M. M Maeda, A. Chang, 2018. Unmanned aerial system assisted framework for the selection of high yielding cotton genotypes. Computers and Electronics in Agriculture. 152: 74-81.

Li, X., W. S. Lee, M. Li, R. Ehsani, A. R. Mishra, C. Yang, et al. 2012. Spectral difference analysis and airborne imaging classification for citrus greening infected trees. Computers and Electronics in Agriculture, 83, 32–46.

Lopez-Granados, F., J. Torres-Sa´nchez, A. Serrano-Pe´rez, A. de Castro,, F. Mesas-Carrascosa, J. Pen˜a,. 2016. Early season weed mapping in sunflower using UAV technology: variability of herbicide treatment maps against weed thresholds. Precision Agriculture, 17(2), 183–199

Maja J.M.J., P. Astillo, T. Campbell, Neto, J. Camargo. 2016. Proceedings of SPIE - The International Society for Optical Engineering, SPIE DOI: 10.1117/12.2228929

Malambo, L., S.C. Popescu, S.C. Murray, E. Putman, N.A. Pugh, D.W. Horne, G. Richardson, R. Sheridan, W.L. Rooney, R. Avant, M. Vidrine, B. McCutchen, D. Baltensperger, M. Bishop, 2018, Multitemporal field-based plant height

estimation using 3D point clouds generated from small unmanned aerial systems high-resolution imagery, Int. J. Appl. Earth Obs. Geoinf. 64, 31–42.

Mao, W., Y. Wang, Y. Wang, 2003. Real-time detection of between-row weeds using machine vision. ASAE paper number 031004. The Society for Agricultural, Food, and Biological Systems, St. Joseph, MI.

Marois, J. J., D. L. Wright, P. J. Wiatrak, and M. A. Vargas. 2004. Effect of row width and nitrogen on cotton morphology and canopy microclimate. Crop Sci. 44: 870–877.

Meng, Y.L, F.J. Lv, W.Q. Zhao, J. Chen, L. Zhu, Y. Wang, B. Chen, Z. Zhou. 2016. Plant density influences fiber sucrose metabolism in relation to cotton fiber quality, Acta Physiol Plant, 38, 112.

Meredith, W.R., Jr., and R.R. Bridge. 1973. The relationship between F2 and selected F3 progenies in cotton (Gossy- pium hirsutum L.). Crop Sci. 13: 354-356.

Moré J.J., 1997. The Levenberg-Marquardt algorithm: implementation and theory, G.A. Watson (Ed.), Numerical Analysis, Lecture Notes in Mathematics 630: 105-116.

Nichols, S.P., C.E. Snipes, and M.A. Jones. 2004. Cotton growth, lint yield, and fiber quality as affected by row spacing and cultivar. J. Cotton Sci. 8:1–12 [Online]. Available at http://www.cotton.org/journal/2004-08/1/ (verified 15 May 2009).

Reddy, K.N. 2001. Broadleaf weed

Nijland W., R. de jong, S.M. de jong, M.A. Wulder, C.W. Bater, N.C. Coops. 2014. Monitoring plant condition and phenology using infrared sensitive consumer Agricultural and Forest Meteorology 184: 98-106.

Norton, E.R., and J.C. Silvertooth. 1999. Development of a Yield Projection Technique for Arizona Cotton. A College of Agriculture Report. Series: 105 -108.

Oosterhuis, D.M., F.M. Bourland, N.P. Tugwell, Cochran, M.J., Danforth, D.M., 2008. Terminology and concepts related to the COTMAN crop monitoring system. In: Oosterhuis, D.M., Bourland, F.M. (Eds.), COTMAN Crop Management System. University of Arkansas: 91–98

Parvin, D. W., S.W. Martin, F. Cooke, and B.B. Freeland. 2005. Effect of Harvest Season Rainfall on Cotton Yield. Journal of Cotton Science 9(3): 1408—1417.

Paterson, A.H., Y. Saranga, M. Menz, C.-X. Jiang, and R. Wright. 2003. QTL analysis of genotype × environment interactions affecting cotton fiber quality. Theor. Appl. Genet 106: 384–396.

Poschlod, P., M.V. Vaieretti, G. Conti, A.C. Staver, S. Aquino, J.H.C. Cornelissen. 2013. New handbook for standardised measurement of plant functional traitsworldwide. Australian J. Botany 61: 167–234.

Rao, N. R., P. K. Garg, S. K. Ghosh, V. K. Dadhwal, 2008. Estimation of leaf total chlorophyll and nitrogen concentrations using hyperspectral satellite imagery. Journal of Agricultural Science (146): 65–75.

Rasmussen, J., J. Nielsen, F. Garcia-Ruiz, S. Christensen, J. C. Streibig. 2013. Potential uses of small unmanned aircraft systems (UAS) in weed research. Weed Research 53(4): 242–248.

Read, J. J., K.R. Reddy, and J.N. Jenkins. 2006. Yield and fiber quality of upland cotton as influenced by nitrogen and potassium nutrition. European Journal of Agronomy 24(3): 282-290.

Sawan, Z. M., M. H. Mahmoud and A. H. El-Guibali. 2006. Response of yield, yield components, and fiber properties of Egyptian cotton (Gossypium barbadense L.) to nitrogen fertilization and foliar-applied potassium and mepiquat chloride. J. Cotton Sci. 10:224-234.

Seelan, S. K., S. Laguette, G. M. Casady, G. A. Seielstad. 2003. Remote sensing applications for precision agriculture: A learning community approach. Remote Sensing of Environment 88:157-169.

Shen X., W. Guo, X. Zhu, Y. Yuan, J. Yu, R. Kohel, T. Zhang. 2005. Molecular mapping of QTLs for fiber qualities in three diverse lines in Upland cotton using SSR markers. Molecular Breed 15:169-181.

Shi, Y., J.A Thomasson, S.C. Murray, N.A. Pugh, W.L. Rooney, S. Shafian, N. Rajan, et al. 2016. Unmanned Aerial Vehicles for High-Throughput Phenotyping and Agronomic Research. Plos One 11.

Shurley, S. Brown, R. McDaniel, B. McNeill, J. Clark, and R. Blackley. 2004. Skip-row cotton performance across multiple yield environments, p. 2284. In Proceedings of the Beltwide Cotton Conferences. National Cotton Council, Memphis, TN.

Smith, B. 1991. A Review of the Relationship of Cotton Maturity and Dyeability. Textile Research Journal 61(3): 137-145.

Smith, C.W., S. Hague, and D. Jones. 2011. Registration of 'Tamcot 73' upland cotton cultivar. Journal of Plant Registrations.5: 273-278.

Snavely N., S.M. Seitz, R. Szeliski. 2008. Modeling the world from internet photo collections. International Journal of Computer Vision 80: 189-210.

Snipes, C. E., C.C. Baskin. 1994. Influence of early defoliation on cotton yield, seed quality, and fiber properties. Field Crop Res. 37: 137-143.

Stafford, J. V. 2000. Implementing precision agriculture in the 21st century. Journal of Agricultural Engineering Research, 76: 267-275.

Sugiura, R., N. Noguchi, K. Ishii. 2005. Remote - sensing technology for vegetation monitoring using an unmanned helicopter. Biosystems Engineering, 90 (4), 369-379.

Sui, R., D. K. Fisher, K. N. Reddy. 2012. Cotton yield assessment using plant height mapping system. The Journal of Agricultural Science 5:23.

Sun, S, C. Li, A. Paterson. 2017. In-field high-throughput phenotyping of cotton plant height using LIDAR. Remote Sens 9: 377.

Tian, M., S. Ban, Q. Chang, M You. 2016. Use of hyperspectral images from UAV-based imaging spectroradiometer to estimate cotton leaf area index. Acta Ecologica Sinica 32(21): 102-108.

Tucker, C. 1979. "Red and Photographic Infrared Linear Combinations for Monitoring Vegetation", Remote Sensing of Environment 8: 127-150.

Westoby, M.J., J. Brasington, N.F. Glasser, M.J. Hambrey, J.M. Reynolds. 2012. 'Structure-from-Motion' photogrammetry: a low-cost, effective tool for geoscience applications. Geomorphology, 179, pp. 300-314

Woebbecke, D.M., G.E. Meyer, K. Von Bargen, and D.A. Mortensen. 1995. Color indices for weed identification under various soil residue and lighting conditions. American Society of Agricultural and Biological Engineers 38: 259-269.

Wu, J. D., D. Wang, M. E. Bauer. 2007. Assessing broadband vegetation indices and QuickBird data in estimating leaf area index of corn and potato canopies. Field Crops Research, 102: 33-42.

Xu, R., C. Li, and A.H. Paterson. 2019. Multispectral imaging and unmanned aerial systems for cotton plant phenotyping. Plos One 14(2).

Yeom, J., J. Jung, A. Chang, M. Maeda, J. Landivar. 2018. Automated Open Cotton Boll Detection for Yield Estimation Using Unmanned Aircraft Vehicle (UAV) Data. Remote Sensing 10(12): 1895.

Zhang, C., and J.M. Kovacs. 2012. The application of small unmanned aerial systems for precision agriculture: a review. Precision Agriculture 13(6): 693-712.

Zhou, X., H. Zheng, X. Xu, J. He, X. Ge, X. Yao, T. Cheng, Y. Zhu, W. Cao, and Y. Tian. 2017. Predicting grain yield in rice using multi-temporal vegetation indices from UAV-based multispectral and digital imagery. ISPRS Journal of Photogrammetry and Remote Sensing 130: 246-255.